

Stopping inward planetary migration by a toroidal magnetic field

Caroline E. J. M. L. J. Terquem

*Institut d’Astrophysique de Paris, 98 bis Boulevard Arago, 75014 Paris, France — terquem@iap.fr
Université Denis Diderot–Paris VII, 2 Place Jussieu, 75251 Paris Cedex 5, France*

Accepted. Received; in original form

ABSTRACT

We calculate the linear torque exerted by a planet on a circular orbit on a disc containing a toroidal magnetic field. All fluid perturbations are singular at the so-called *magnetic resonances*, where the Doppler shifted frequency of the perturbation matches that of a slow MHD wave propagating along the field line. These lie on both sides of the corotation radius. Waves propagate outside the Lindblad resonances, and also in a restricted region around the magnetic resonances.

The magnetic resonances contribute to a significant global torque which, like the Lindblad torque, is negative (positive) inside (outside) the planet’s orbit. Since these resonances are closer to the planet than the Lindblad resonances, the torque they contribute dominates over the Lindblad torque if the magnetic field is large enough. In addition, if $\beta \equiv c^2/v_A^2$ increases fast enough with radius, the outer magnetic resonance becomes less important and the total torque is then negative, dominated by the inner magnetic resonance. This leads to outward migration of the planet. Even for $\beta \sim 100$ at corotation, a negative torque may be obtained. A planet migrating inward through a nonmagnetized region of a disc would then stall when reaching a magnetized region. It would then be able to grow to become a terrestrial planet or the core of a giant planet. In a turbulent magnetized disc in which the large scale field structure changes sufficiently slowly, a planet may alternate between inward and outward migration, depending on the gradients of the field encountered. Its migration could then become diffusive, or be limited only to small scales.

Key words: accretion, accretion discs – MHD – waves – planetary systems: protoplanetary discs

1 INTRODUCTION

Almost 20% of the extrasolar planets detected so far orbit at a distance between 0.038 and 0.1 astronomical unit (au) from their host star. It is very unlikely that these short-period giant planets, also called ‘hot Jupiters’, have formed *in situ* (Bodenheimer 1998; Bodenheimer, Hubickyj & Lissauer 1999). More likely, they have formed further away in the protoplanetary nebula and have migrated down to small orbital distances. It is also possible that migration and formation were concurrent (Papaloizou & Terquem 1999).

So far, three mechanisms have been proposed to explain the location of planets at very short orbital distances. One of them relies on the gravitational interaction between two or more giant planets, which may lead to orbit crossing and to the ejection of one planet while the other is left in a smaller orbit (Rasio & Ford 1996; Weidenschilling & Marzari 1996). However, this mechanism cannot account for the relatively large number of hot Jupiters observed. Another mechanism is the so-called ‘migration instability’ (Murray et al. 1998; Malhotra 1993). It involves resonant interactions between the planet and planetesimals located inside its orbit which lead to the ejection of a fraction of them while simultaneously causing the planet to migrate inward. Although such interactions may lead to the migration of giant planets on small scales, they would require a very massive disc to move a Jupiter mass planet from several astronomical units down to very small radii. Such a massive disc is unlikely and furthermore it would be only marginally gravitationally stable. The third mechanism, that we are going to focus on here, involves the tidal interaction between the protoplanet and the gas in the surrounding protoplanetary nebula (Goldreich & Tremaine 1979, 1980; Lin & Papaloizou 1979, 1993 and references therein; Papaloizou & Lin 1984; Ward 1986, 1997). Here again the protoplanet can move significantly only if there is at least a comparable mass of gas within a radius comparable to that of its orbit. However this is not a problem since this amount of gas is needed anyway in the first place to form the planet.

2 Caroline Terquem

Note that hot Jupiters can also be produced by the dynamical relaxation of a population of planets on inclined orbits, formed through gravitational instabilities of a circumstellar envelope or a thick disc (Papaloizou & Terquem 2001). However, if objects as heavy as τ -Boo may be produced *via* fragmentation, it is unlikely that lower mass objects would form that way.

A planet embedded in a gaseous disc launches density waves at the Lindblad resonances (Goldreich & Tremaine 1979, hereafter GT79). The torque exerted by the planet on these waves is responsible for the exchange of angular momentum between the disc rotation and the planet's orbital motion. The interaction between the planet and the disc inside/outside its orbit leads to a negative/positive torque on the disc, and therefore to a gain/loss of angular momentum for the planet. In the linear regime, because in a (even uniform) Keplerian disc the outer Lindblad resonances are slightly closer to the planet than the inner Lindblad resonances, the interaction with the outer parts of the disc leads to a larger Lindblad torque than that with the inner parts (Ward 1986, 1997). Therefore, the net Lindblad torque exerted by the planet causes it to lose angular momentum and to move inward relative to the gas (type I migration). Note that there is also a torque exerted by the planet on the material which corotates with the perturbation. Its sign depends on the gradient of vortensity at corotation (GT79). However, it is usually found to be less significant than the net Lindblad torque. The drift timescale for a $1-10 M_{\oplus}$ planet undergoing type I migration in a standard gaseous disc is typically between 10^4 and 10^6 years, shorter than the disc lifetime or estimated planetary formation timescales.

When the mass of the planet becomes large enough, the perturbation becomes nonlinear. Feedback torques from the disc on the planet, which have to be taken into account in this regime, then opposes the motion of the planet and stops it altogether when the planet is massive enough (Ward 1997). However, density waves still transport angular momentum outward. If they are dissipated locally, the angular momentum they transport is deposited in the disc in the vicinity of the planet and a gap may be cleared out (Goldreich & Tremaine 1980; Lin & Papaloizou 1979, 1993 and references therein). The planet is then locked into the angular momentum transport process of the disc, and migrates inward at a rate controlled by the disc viscous timescale (type II migration). Here again, the drift timescale is rather short, being in the range 10^3-10^5 years for standard parameters.

Type II migration, which occurs for planets with masses at least comparable to that of Jupiter, can be avoided if after the planet forms there is not enough mass left in the disc to absorb its angular momentum. However, type I migration appears inevitable as there has to be enough gas in the disc to push a forming core inward if this core is to accrete a massive envelope to become a giant planet at some point. Different scenarios for stopping a planet undergoing inward migration have been considered (see, e.g., Terquem, Papaloizou & Nelson 2000 and references therein), but none of them can satisfactorily explain the presence of extrasolar planets with semi-major axes from a few 0.01 au all the way up to several au.

Recently, Papaloizou (2002) has shown that type I migration reverses for reasonable disc models once the eccentricity of the orbit becomes comparable to the disc aspect ratio. This is because in that case the planet spends more time near apocentre, where it is being speeded up, than near pericentre, where it is being slowed down. Although the interaction with the disc tends to circularize the orbit of the planet (Goldreich & Tremaine 1980), significant eccentricity may be maintained by gravitational interactions between different planets forming simultaneously (Papaloizou & Larwood 2000).

Here we investigate the effect of a magnetic field on planet migration in the linear regime. We consider a planet on a circular orbit and, to keep the problem tractable, restrict ourselves to the case of a purely toroidal field. This tends to be the dominant component in discs as it is produced by the shearing of radial field lines. As described above, the torque exerted by a planet on a disc depends mainly on the location of the radii where the perturbation is in resonance with the free oscillations of the disc. We therefore expect a magnetic field to modify the tidal torque, as it introduces more degrees of freedom in the disc.

The plan of the paper is as follows. In sections 2, 3 and 4 we give the basic equations, describe the equilibrium disc model and give the expression of the perturbing potential acting on the disc. In section 5 we study the disc response to this perturbing potential. We first linearize the equations and derive the second order differential equation describing the disc response (§ 5.1). We then carry on a WKB analysis (§ 5.2), which shows that magnetosonic waves propagate outside the outermost turning points. In § 5.3 we study the disc response at the locations where it is singular. We call these radii *magnetic resonances*. There are two such resonances, located on each side of the planet's orbit and within the Lindblad resonances. In § 5.4 we calculate all the turning points associated with the disc response. On each side of the planet there are two or three of them, depending on the value of the azimuthal number m . One of these turning points coincide with the Lindblad resonance. In contrast to the nonmagnetic case, waves are found to propagate in a restricted region inside the outermost turning points, around the magnetic resonances. We then proceed to give an expression for the tidal torque in general and in the vicinity of the magnetic resonances in particular in section 6. Numerical calculations of the torque exerted by the planet on the disc are presented in section 7. We show that the torque exerted in the vicinity of the magnetic resonances tends to dominate the disc response when the magnetic field is large enough. This torque, like the Lindblad torque, is negative inside the planet's orbit and positive outside the orbit. Therefore, if $\beta \equiv c^2/v_A^2$ increases fast enough with radius, the outer magnetic resonance becomes less important (it disappears altogether when there is no magnetic field outside the planet's orbit) and the total torque becomes negative, dominated by the inner magnetic resonance. This corresponds to a positive torque on the planet, which leads to outward migration. Finally, we discuss our results in section 8.

2 BASIC EQUATIONS

The disc is described by the equation of motion:

$$\rho \left(\frac{\partial \mathbf{v}}{\partial t} + (\mathbf{v} \cdot \nabla) \mathbf{v} \right) = -\nabla P + \mathbf{F} - \rho \nabla \Psi, \quad (1)$$

the equation of continuity:

$$\frac{\partial \rho}{\partial t} + \nabla \cdot (\rho \mathbf{v}) = 0, \quad (2)$$

and the induction equation in the ideal MHD approximation:

$$\frac{\partial \mathbf{B}}{\partial t} = \nabla \times (\mathbf{v} \times \mathbf{B}), \quad (3)$$

where

$$\mathbf{F} = \frac{1}{\mu_0} (\nabla \times \mathbf{B}) \times \mathbf{B} \quad (4)$$

is the Lorentz force per unit volume, P the pressure, ρ the mass density, \mathbf{v} the flow velocity, Ψ the gravitational potential and \mathbf{B} the magnetic field (μ_0 is the permeability of vacuum). SI units are used throughout the paper. Here we neglect self gravity so that the gravitational potential Ψ is assumed to be due to a central mass M_* .

We consider a thin disc, so that the above equations can be averaged over the disc thickness. To first order we neglect the z -dependence of \mathbf{v} and Ψ , so that the vertically averaged equation of motion and continuity are, respectively:

$$\Sigma \left[\frac{\partial \mathbf{v}}{\partial t} + (\mathbf{v} \cdot \nabla) \mathbf{v} \right] = -\nabla \langle P \rangle + \langle \mathbf{F} \rangle - \Sigma \nabla \Psi, \quad (5)$$

$$\frac{\partial \Sigma}{\partial t} + \nabla \cdot (\Sigma \mathbf{v}) = 0, \quad (6)$$

where Σ is the surface mass density and the brackets denote averaging over the disc thickness.

To close the system of equations, we adopt a barotropic equation of state:

$$\langle P \rangle = \langle P \rangle (\Sigma). \quad (7)$$

The sound speed c is then given by:

$$c^2 = \frac{d\langle P \rangle}{d\Sigma}. \quad (8)$$

3 EQUILIBRIUM DISC STRUCTURE

We adopt a nonrotating cylindrical polar coordinate system (r, φ, z) with origin at the central mass. We denote $(\mathbf{e}_r, \mathbf{e}_\varphi, \mathbf{e}_z)$ the associated unit vectors. We suppose that at equilibrium the disc is axisymmetric and in rotation around a central mass, so that $\mathbf{v} = (0, r\Omega(r), 0)$, where Ω is the angular velocity. Furthermore, we assume that the equilibrium configuration contains only a toroidal magnetic field, i.e. $\mathbf{B} = (0, B(r, z), 0)$. The Lorentz force per unit volume is then:

$$\mathbf{F} = \frac{1}{\mu_0} \left(-\frac{B}{r} \frac{\partial (rB)}{\partial r}, 0, -B \frac{\partial B}{\partial z} \right). \quad (9)$$

If we assume reflection with respect to the disc midplane and that B vanishes at the disc surface, this leads to:

$$\langle \mathbf{F} \rangle = \frac{1}{\mu_0} \left(-\frac{1}{2r^2} \frac{d}{dr} (r^2 \langle B^2 \rangle), 0, 0 \right). \quad (10)$$

4 PERTURBING POTENTIAL

We consider a planet of mass $M_p \ll M_*$ on a circular orbit with radius r_p and angular velocity $\Omega_p = \sqrt{GM_*/r_p^3}$. At the location (r, φ) in the disc, it exerts the gravitational potential:

$$\Psi'_p(r, \varphi, t) = \Psi'_p(r, \phi) = -\frac{GM_p}{(r_0^2 + r_p^2 + r^2 - 2rr_p \cos \phi)^{1/2}}, \quad (11)$$

where $\phi = \varphi - \Omega_p t$ and we have introduced a softening length r_0 . We now expand Ψ'_p in a Fourier series with respect to the variable ϕ :

$$\Psi'_p(r, \phi) = \sum_{m=0}^{\infty} \Psi'_m(r) \cos m\phi, \quad (12)$$

with

$$\Psi'_{m \neq 0}(r) = \frac{2}{\pi} \int_0^\pi \Psi'_p(r, \phi) \cos m\phi d\phi,$$

and

$$\Psi'_0(r) = \frac{1}{\pi} \int_0^\pi \Psi'_p(r, \phi) d\phi.$$

Using the generalized Laplace coefficients defined as (Ward 1989; Korycansky & Pollack 93, hereafter KP93):

$$b_{1/2}^m(\gamma) = \frac{2}{\pi} \int_0^\pi \frac{\cos m\phi d\phi}{(q^2 + p^2\gamma^2 - 2\gamma \cos \phi)^{1/2}}, \quad (13)$$

where:

$$\text{if } r < r_p : \gamma = \frac{r}{r_p}, \quad p = 1, \quad q^2 = 1 + \frac{r_0^2}{r_p^2},$$

$$\text{if } r > r_p : \gamma = \frac{r_p}{r}, \quad q = 1, \quad p^2 = 1 + \frac{r_0^2}{r_p^2},$$

we can rewrite Ψ'_m under the form:

$$\frac{\Psi'_{m \neq 0}}{r_p^2 \Omega_p^2} = -\frac{M_p}{M_*} \frac{r_p}{r} b_{1/2}^m(\gamma) \quad \text{if } r > r_p, \quad (14)$$

$$\frac{\Psi'_{m \neq 0}}{r_p^2 \Omega_p^2} = -\frac{M_p}{M_*} b_{1/2}^m(\gamma) \quad \text{if } r < r_p, \quad (15)$$

and the expression on the right-hand-side has to be divided by a factor two if $m = 0$. The subscript 'p' indicates that the quantities have to be evaluated at $r = r_p$.

5 THE DISC RESPONSE

5.1 Linearization of the basic equations

In this paper we consider small perturbations, so that the basic equations can be linearized. We denote Eulerian perturbations with a prime. Since the equilibrium is axisymmetric and steady, we can expand each of the perturbed quantities in Fourier series with respect to the variable ϕ and solve separately for each value of m . The general problem may then be reduced to calculating the response of the disc to the real part of a complex potential of the form $\Psi'_m(r)\exp[i(m\varphi - \omega t)]$, where the amplitude Ψ'_m is real and the frequency $\omega \equiv m\Omega_p$, and summing up over m . We make all Eulerian fluid state variable perturbations complex by writing:

$$X'(r, \varphi, t) = \sum_{m=0}^{\infty} X'_m(r) e^{i(m\varphi - \omega t)}, \quad (16)$$

where X is any state variable. The physical perturbations will be recovered by taking the real part of these complex quantities. We denote ξ the Lagrangian displacement, and write its m -th Fourier component as $\xi_m(r)\exp[i(m\varphi - \omega t)]$. Since here we are only interested in the perturbations induced by the planet in the plane of the disc, we take $\xi_z = 0$.

Linearization of the induction equation (3), or the equivalent statement of the conservation of magnetic flux, leads to an expression for the perturbed magnetic field in the form (Chandrasekhar & Fermi 1953):

$$\mathbf{B}' = \nabla \times (\xi \times \mathbf{B}). \quad (17)$$

The corresponding perturbation of the Lorentz force per unit volume is:

$$\mathbf{F}' = \frac{1}{\mu_0} [(\nabla \times \mathbf{B}') \times \mathbf{B} + (\nabla \times \mathbf{B}) \times \mathbf{B}']. \quad (18)$$

Use of equations (17) and (18) with $\xi_z = 0$ gives:

$$\langle F'_{mr} \rangle = \frac{\langle B^2 \rangle}{\mu_0 r} \left[r \frac{d^2 \xi_{mr}}{dr^2} + \left(\frac{3b_1}{2} - 1 \right) \frac{d\xi_{mr}}{dr} + \left(\frac{b_2}{2} - m^2 \right) \frac{\xi_{mr}}{r} \right], \quad (19)$$

$$\langle F'_{m\varphi} \rangle = \frac{imb_1}{2\mu_0} \frac{\langle B^2 \rangle \xi_{mr}}{r^2}, \quad (20)$$

$$\langle F'_{mz} \rangle = 0, \quad (21)$$

where we have defined the dimensionless quantities:

$$b_1 \equiv \frac{d \ln (r^2 \langle B^2 \rangle)}{d \ln r}, \quad b_2 \equiv \frac{1}{\langle B^2 \rangle} \frac{d}{dr} \left(r^2 \frac{d \langle B^2 \rangle}{dr} \right). \quad (22)$$

We now linearize the r - and φ -components of the equation of motion (5) and the equation of continuity (6). Using $v'_{mr} = im\sigma\xi_{mr}$, with $\sigma \equiv \Omega - \Omega_p$, and equations (7) and (8), we get:

$$-m^2\sigma^2\xi_{mr} - 2\Omega v'_{m\varphi} = -\frac{d}{dr}(\Psi'_m + W'_m) + \frac{1}{\Sigma} \left(-\frac{W'_m}{c^2} \langle F_r \rangle + \langle F'_{mr} \rangle \right), \quad (23)$$

$$\sigma v'_{m\varphi} + \frac{\sigma\kappa^2}{2\Omega}\xi_{mr} = -\frac{1}{r}(\Psi'_m + W'_m) - \frac{i}{m\Sigma} \langle F'_{m\varphi} \rangle, \quad (24)$$

$$\frac{\sigma W'_m}{c^2} = -\frac{1}{r\Sigma} \frac{d}{dr}(r\sigma\Sigma\xi_{mr}) - \frac{v'_{m\varphi}}{r}, \quad (25)$$

where we have found it convenient to use the radial component of the Lagrangian displacement ξ_{mr} and the azimuthal component of the Eulerian perturbed velocity $v'_{m\varphi}$ as variables. Here $W' = \Sigma'c^2/\Sigma$ is the linear perturbation of the enthalpy and κ is the epicyclic frequency, which is defined by:

$$\kappa^2 = \frac{2\Omega}{r} \frac{d(r^2\Omega)}{dr}.$$

We can further eliminate $v'_{m\varphi}$ and W'_m to get, after some tedious algebra, the following second-order differential equation for ξ_{mr} :

$$\mathcal{A}_2 \frac{d^2\xi_{mr}}{dr^2} + \frac{\mathcal{A}_1}{r} \frac{d\xi_{mr}}{dr} + \mathcal{A}_0 \frac{\xi_{mr}}{r^2} = \frac{1}{c^2} \frac{d\Psi'_m}{dr} - \mathcal{S}_0 \Psi'_m, \quad (26)$$

with:

$$\mathcal{A}_2 = 1 + \frac{1}{\beta} \left(1 - \frac{c^2}{r^2\sigma^2} \right), \quad (27)$$

$$\mathcal{A}_1 = \frac{2c^2}{r^2\sigma^2 - c^2} \left(-1 - \frac{\kappa^2}{2\Omega\sigma} + \frac{2\Omega}{\sigma} + \frac{r^2\sigma^2}{c^2} c_1 \right) + 1 + d_1 + \frac{b_1 - 1}{\beta} \left(1 - \frac{c^2}{r^2\sigma^2} \right), \quad (28)$$

$$\begin{aligned} \mathcal{A}_0 = & \frac{r^2\sigma^2}{c^2} \left(m^2 - \frac{\kappa^2}{\sigma^2} \right) - d_1^2 + d_2 + 1 - m^2 + 2c_1d_1 + \frac{2\Omega}{\sigma} d_1 \\ & + \frac{2r^2\sigma^2}{r^2\sigma^2 - c^2} \left(-\frac{\kappa^2}{2\Omega\sigma} + \frac{2\Omega}{\sigma} - 1 + c_1 \right) \left(1 - \frac{2\Omega}{\sigma} + \frac{c^2}{r^2\sigma^2} d_1 \right) \\ & + \frac{1}{\beta} \left\{ b_1 \left[\frac{2\Omega}{\sigma} - \frac{1}{2} - \frac{d_1}{2} \left(1 + \frac{c^2}{r^2\sigma^2} \right) + \frac{c^2}{r^2\sigma^2 - c^2} \left(-\frac{\kappa^2}{2\Omega\sigma} + \frac{2\Omega}{\sigma} - 1 + c_1 \right) \right] \right. \\ & \left. + \frac{b_2}{2} - m^2 + \frac{c^2}{r^2\sigma^2} (m^2 - 1) - \frac{b_1^2 c^2}{4\beta r^2\sigma^2} \right\}, \end{aligned} \quad (29)$$

$$\mathcal{S}_0 = \frac{1}{r^3\sigma^2} \left[\frac{2r^2\sigma^2}{r^2\sigma^2 - c^2} \left(\frac{\kappa^2}{2\Omega\sigma} - \frac{2\Omega}{\sigma} + 1 - c_1 \right) - \frac{2r^2\Omega\sigma}{c^2} + \frac{b_1}{2\beta} \right], \quad (30)$$

where $\beta \equiv c^2/v_A^2$, with $v_A \equiv \sqrt{\langle B^2 \rangle / (\mu_0\Sigma)}$ being the Alfvén speed, and we have defined the dimensionless quantities:

$$d_1 \equiv \frac{d \ln \Sigma}{d \ln r}, \quad d_2 \equiv \frac{r^2}{\Sigma} \frac{d^2\Sigma}{dr^2}, \quad c_1 \equiv \frac{d \ln c}{d \ln r}. \quad (31)$$

The magnetic field comes in through the parameter β only.

We see by multiplying all the coefficients of equation (26) by σ^2 that there is no singularity in the coefficients of this equation where $\sigma = 0$, i.e. at corotation, in contrast to the nonmagnetic case (GT79). When there is no magnetic field, the particles located at corotation can respond secularly to a forcing with frequency $\Omega = \Omega_p$ and therefore stay exactly in phase with the perturbation (they 'surf' the tidal wave). In the presence of a toroidal field however, the tension of the field line to which the particles are attached provides a restoring force which introduces some inertia in the response of the particles, destroying the resonance.

From equations (20), (24) and (25), we can write W'_m and $v'_{m\varphi}$ as functions of ξ_{mr} . We give these expressions as they will be needed below:

$$W'_m = \frac{r^2\sigma^2c^2}{r^2\sigma^2 - c^2} \left[-\frac{d\xi_{mr}}{dr} + \mathcal{C} \frac{\xi_{mr}}{r} + \frac{\Psi'_m}{r^2\sigma^2} \right], \quad (32)$$

with:

$$\mathcal{C} = -\frac{d}{d \ln r} [\ln(\Sigma r\sigma)] + \frac{\kappa^2}{2\Omega\sigma} - \frac{b_1 c^2}{2\beta r^2\sigma^2}, \quad (33)$$

and:

$$v'_{m\varphi} = \frac{r^2\sigma^2 c}{r^2\sigma^2 - c^2} \left[\frac{c}{r\sigma} \frac{d\xi_{mr}}{dr} + \mathcal{D} \frac{\xi_{mr}}{r} - \frac{\Psi'_m}{r\sigma c} \right], \quad (34)$$

with:

$$\mathcal{D} = \frac{c}{r\sigma} \left\{ \frac{d}{d \ln r} [\ln(\Sigma r\sigma)] + \frac{b_1}{2\beta} \right\} - \frac{\kappa^2 r}{2\Omega c}. \quad (35)$$

5.2 WKB dispersion relation

We assume that the first-order derivative term in equation (26) can be neglected (this is verified *a posteriori*) and we define $x \equiv r/r_p - 1$, where r_p is the corotation radius, i.e., for a circular orbit, the planet orbital radius. Then the homogeneous equation associated with equation (26) can be rewritten as:

$$\left[1 + \frac{1}{\beta} \left(1 - \frac{c^2}{r^2\sigma^2} \right) \right] \frac{d^2}{dx^2} \left(\frac{\xi_{mr}}{r_p} \right) + \frac{\mathcal{A}_0}{(1+x)^2} \frac{\xi_{mr}}{r_p} = 0. \quad (36)$$

We assume $|x| \ll 1$ and $c \ll r|\sigma|$, which means $|x| \gg H/r$, where $H \sim c/\Omega$ is the disc semi-thickness, and $\beta \sim 1$. With $1+x$ being typically on the order of unity, the WKB approximation can then be used if $|\mathcal{A}_0| \gg 1$. We have:

$$\mathcal{A}_0 \simeq \frac{r^2\sigma^2}{c^2} (m^2 - \kappa^2/\sigma^2),$$

providing $1 - \kappa^2/(m^2\sigma^2) \gg c^2/(r^2\sigma^2)$, i.e. $x^2 \gg H^2/r^2 + 1/m^2$. When this condition is satisfied then $|\mathcal{A}_0| \gg 1$ and we may look for homogeneous free-wave solutions of the form $\xi_{mr}(r) = A(r)e^{ikr}$, where $kr \gg 1$ and A is a slowly varying amplitude. Since \mathcal{A}_1 is of order $(H/r)^2 x^{-3}$, the first-order derivative term can be neglected compared to the second-order derivative term in equation (26) if $x^3 \gg (H/r)^2 (kr)^{-1}$. When this is satisfied, the assumption made in this subsection is validated. Then equation (36) yields:

$$k = \pm \sqrt{\frac{m^2\sigma^2 - \kappa^2}{c^2 + v_A^2}}, \quad (37)$$

which is the dispersion relation for magnetosonic waves (e.g., Tagger et al. 1990) propagating outside the Lindblad resonances (located at $r = r_L$ where $m^2\sigma^2 - \kappa^2 = 0$) with the group velocity:

$$v_g = -\frac{k(c^2 + v_A^2)}{m\sigma}. \quad (38)$$

In the absence of magnetic field, these waves reduce to density waves (GT79).

These solutions describe the response of the disc in the parts where the perturbing potential is negligible, i.e. outside the Lindblad resonances and far enough from them.

We now consider the response of the disc inside the Lindblad resonances.

5.3 Magnetic resonances

The differential equation (26) is singular at the radii r_M where \mathcal{A}_2 vanishes, i.e. where $1 + [1 - c^2/(r^2\sigma^2)]/\beta = 0$. We call these locations *magnetic resonances*. There are two such radii, the *inner* magnetic resonance $r_{IMR} < r_p$ and the *outer* magnetic resonance $r_{OMR} > r_p$. At these locations:

$$m^2(\Omega - \Omega_p)^2 = \frac{m^2 c^2 v_A^2}{r^2(v_A^2 + c^2)}, \quad (39)$$

i.e. the frequency of the perturbation in a frame rotating with the fluid matches that of a slow MHD wave propagating along the field line.

Using $\Omega = \Omega_K [1 + \mathcal{O}(H^2/r^2)]$, where Ω_K is the Keplerian angular velocity, and $H/r \ll 1$ we get, to first order in H/r :

$$|r_M - r_p| = \frac{2H}{3\sqrt{1+\beta}}, \quad (40)$$

where H and β are evaluated in the vicinity of r_p . We suppose here that these quantities vary on a scale large compared to H . As the field becomes weaker ($\beta \rightarrow \infty$), the magnetic resonances converge toward the corotation radius. Note that since the effective Lindblad resonances are all located beyond $2H/3$ from corotation (see section 5.4), they are beyond the magnetic resonances.

We define the new variable $x \equiv (r - r_M)/r_M$, where r_M is either the inner or outer resonance, and we do a local analysis of equation (26) around $x = 0$. For $|x| \ll 1$, we have $\mathcal{A}_2 \simeq (d\mathcal{A}_2/dr)_{r=r_M}(r - r_M)$. Here we assume that $h \equiv c/(r\Omega) \sim H/r \ll 1$, the parameters b_1, b_2, c_1, d_1 and d_2 are at most of order unity and $\beta \sim 1$. This amounts to assuming that only σ varies in the expression (27) of \mathcal{A}_2 . For $|x| \ll 1$, we then have:

$$\mathcal{A}_2 \simeq 2\epsilon \frac{(1 + \beta_M)^{3/2}}{\beta_M} \left(-\frac{d \ln \Omega}{d \ln r} \right)_{r_M} \frac{x}{h_M}, \quad (41)$$

where the subscript M indicates that the corresponding quantities are taken at $r = r_M$, and $\epsilon = -1$ or $+1$ depending on whether $r_M = r_{IMR}$ or r_{OMR} .

We now approximate \mathcal{A}_1 , \mathcal{A}_0 and \mathcal{S}_0 by their values at $r = r_M$. This requires $|x| \ll h_M$. If this condition is not satisfied, $\Omega - \Omega_p$ cannot be replaced by its value at $r = r_M$. To the first non zero order in h_M and allowing for $m \sim h_M^{-1}$, we can then rewrite equation (26) under the form:

$$x \frac{\partial^2 \tilde{\xi}_{mr}}{\partial x^2} + \frac{\partial \tilde{\xi}_{mr}}{\partial x} + \mathcal{A} \tilde{\xi}_{mr} = \mathcal{S}, \quad (42)$$

where we have defined the dimensionless quantity $\tilde{\xi}_{mr} \equiv \xi_{mr}/r_M$ and where \mathcal{A} and \mathcal{S} are given by:

$$\mathcal{A} = \frac{\epsilon \beta_M}{3(1 + \beta_M)^{3/2} h_M} \left(\frac{m^2 h_M^2}{1 + \beta_M} + 5 + \frac{6}{\beta_M} \right), \quad (43)$$

$$\mathcal{S} = \frac{1}{3(1 + \beta_M) h_M} \left[\frac{\epsilon \beta_M}{(1 + \beta_M)^{1/2}} \left(\frac{1}{r^2 \Omega^2} \frac{\partial \Psi'_m}{\partial x} \right)_{x=0} + \frac{3 + \beta_M}{h_M} \left(\frac{\Psi'_m}{r^2 \Omega^2} \right)_{x=0} \right]. \quad (44)$$

We next introduce the new variable $u = 2\sqrt{\mathcal{A}x}$, so that equation (42) becomes:

$$\frac{\partial^2 \tilde{\xi}_{mr}}{\partial u^2} + \frac{1}{u} \frac{\partial \tilde{\xi}_{mr}}{\partial u} + \tilde{\xi}_{mr} = \frac{\mathcal{S}}{\mathcal{A}}. \quad (45)$$

Note that u is real outside the magnetic resonances, where $\mathcal{A}x > 0$, whereas it is imaginary inside the resonances, where $\mathcal{A}x < 0$. The solutions of this equation can be written as:

$$\tilde{\xi}_{mr}(u) = \frac{\mathcal{S}}{\mathcal{A}} + \frac{\pi}{2} C_\epsilon Y_0(u) + C'_\epsilon J_0(u), \quad (46)$$

where J_0 and Y_0 are the Bessel functions of first and second kind, respectively, and C_ϵ and C'_ϵ are (complex) constants which *a priori* depend on β_M , h_M and m . The factor $\pi/2$ has been introduced to simplify the asymptotic expression of $\tilde{\xi}$ below.

When $u \rightarrow 0$ (i.e. $|x| \ll h_M$), $J_0(u) \sim 1$ and $Y_0(u) \sim (2/\pi) \ln u$ (Abramowitz & Stegun 1972). To deal with the singularity at $u = 0$, we use the Landau prescription, i.e. we displace the pole slightly from the real axis by replacing $\Omega - \Omega_p$ with $\Omega - \Omega_p - i\Gamma$, where Γ is a small positive real constant. This amounts to multiplying all the perturbed quantities by $\exp(\Gamma t)$, and therefore to considering the response of the disc to a slowly increasing perturbation. This procedure can also be thought of as introducing a viscous force, or as shifting the resonances progressively with time. Note that such a shift occurs when the planet drifts through the disc, since the material in the resonances then changes with time. Shifting $\Omega - \Omega_p$ below the real axis is equivalent to shifting x above this axis in equation (42), since only $\Omega - \Omega_p$ was allowed to vary in the expression of \mathcal{A}_2 . Therefore, we replace x with $x + i\gamma$, where γ is a small positive real constant. For $|x| \ll h_M$, the solutions of equation (45) can then be written as:

$$\tilde{\xi}_{mr} \simeq C_\epsilon \ln [4\mathcal{A}(x + i\gamma)], \quad (47)$$

so that, near $x = 0$:

$$\tilde{\xi}_{mr} \simeq C_\epsilon \left(\ln |4\mathcal{A}\gamma| + i \arctan \frac{\gamma}{x} \right). \quad (48)$$

Note that there is a phase shift of π on passing through $x = 0$.

Since \mathcal{S}/\mathcal{A} has opposite sign at $r = r_{IMR}$ and $r = r_{OMR}$ ($\partial \Psi'_m / \partial x$ changes sign on passing through corotation whereas Ψ'_m does not) and is real, the real part of the solutions of equation (45) should have opposite sign at $r = r_{IMR}$ and $r = r_{OMR}$ whereas their imaginary parts should have the same sign. Therefore, from equation (48) we get $C_{+1} = -C_{-1}^*$, where the asterisk denotes the complex conjugate.

Equations (32) and (34) can now be used to evaluate $v'_{m\varphi}$ and W'_m for $|x| \ll h_M$:

$$\frac{W'_m}{r_M^2 \Omega_M^2} \simeq C_\epsilon \frac{h_M^2}{\beta_M (x + i\gamma)}, \quad (49)$$

$$\frac{v'_{m\varphi}}{r_M \Omega_M} \simeq \epsilon C_\epsilon \frac{(1 + \beta_M)^{1/2} h_M}{\beta_M (x + i\gamma)}, \quad (50)$$

where Ω_M is Ω taken at $r = r_M$. Finally, $v'_{mr} = im\sigma \tilde{\xi}_{mr}$ yields, for $|x| \ll h_M$:

$$\frac{v'_{mr}}{r_M \Omega_M} \simeq -\epsilon i C_\epsilon \frac{mh_M}{(1 + \beta_M)^{1/2}} \ln [4\mathcal{A}(x + i\gamma)]. \quad (51)$$

We note that, in a nonmagnetized disc, the azimuthal perturbed velocity varies as $\ln x$ with $x = |r - r_p|/r_p \rightarrow 0$ near corotation (GT79), whereas here it varies as $1/x$ near the magnetic resonances.

5.4 Turning points

At the locations where the solutions of equation (26) change from wave-like to non wave-like (turning points), the disc response varies on a large scale, and therefore it couples well to the perturbing potential. This results in a large contribution to the tidal torque (see GT79 and § 6). It is therefore important to calculate the location of these turning points.

The WKB analysis above (see § 5.2) indicates that the differential equation (26) has turning points at the locations of the so-called *nominal* Lindblad resonances $r = r_L$. Waves propagate outside these resonances, which are located on both sides of the corotation radius. In the nonmagnetic case, it is known that the turning points do no coincide with the nominal Lindblad resonances for values of m in excess of r/H (Goldreich & Tremaine 1980, Artymowicz 1993). If they did coincide, the turning points (also called *effective* Lindblad resonances) would converge toward r_p as m increases. Instead, they converge toward a radius which is located a finite distance (equal to $2H/3$) away from r_p . Since the potential is more and more localized around r_p at large m , coupling between the perturbation and the disc response is lost, and the contribution to the total torque becomes negligible. This is the torque cutoff first discussed by Goldreich & Tremaine (1980).

The WKB analysis above indicates that for values of m up to about r/H , the location of the turning points does not depend on whether there is a magnetic field or not. In both cases they coincide with the nominal Lindblad resonances. However, for larger values of m , there are differences between a magnetized and a nonmagnetized disc, as the analysis below shows. We now calculate the location of the turning points.

5.4.1 Elimination of the first-order derivative term in equation (26):

There are no singularities in the coefficients of equation (26) at $r = r_L$. This is similar to the nonmagnetic case, where only the second-order differential equation for W'_m has (removable) singularities there (Narayan, Goldreich & Goodman 1987). All the physical quantities are regular at these locations. To identify the turning points, we eliminate the first-order derivative term in this equation. We define $x \equiv (r - r_L)/r_L$, r_L being either the inner or outer nominal Lindblad resonance, and introduce the new dependent variable:

$$y = \xi_{mr} \exp\left(\frac{1}{2} \int \frac{\mathcal{A}_1}{\mathcal{A}_2} dx\right), \quad (52)$$

so that the homogeneous equation associated with equation (26) can be written under the exact form:

$$\frac{d^2y}{dx^2} + \mathcal{K}y = 0, \quad (53)$$

where:

$$\mathcal{K} = \frac{\mathcal{A}_0}{\mathcal{A}_2} - \frac{1}{4} \left(\frac{\mathcal{A}_1}{\mathcal{A}_2}\right)^2 - \frac{1}{2} \frac{d}{dx} \left(\frac{\mathcal{A}_1}{\mathcal{A}_2}\right). \quad (54)$$

We now expand \mathcal{K} around $x = 0$. At $r = r_L$, $\kappa^2 = m^2\sigma^2$. We neglect here the departure from Keplerian rotation (which is second order in H/r) so that $\kappa = \Omega$. Then $\sigma = \epsilon\Omega(r_L)X/m$, with $X = 1 + 3\epsilon mx/2$ and $\epsilon = +1$ or -1 depending on whether we consider the outer or inner resonance, respectively. We assume β and $h \equiv c/(r\Omega) \sim H/r$ constant. Note that for values of $m \sim 1/h$ and for $x \sim h$, we cannot approximate σ by its value at r_L . After some algebra, we find, to the first non zero order:

$$\begin{aligned} \frac{m^2}{\mathcal{A}_2^2} \mathcal{K} = & \frac{X^2 - 1}{m^2 h^2} - 1 - \frac{6}{X^2 - m^2 h^2} - \frac{27}{4} \frac{m^2 h^2}{(X^2 - m^2 h^2)^2} \\ & + \frac{1}{\beta} \left\{ \left(1 - \frac{m^2 h^2}{X^2}\right) \left[\frac{X^2 - 1}{m^2 h^2} - 2 - \frac{6}{X^2 - m^2 h^2} - \frac{1}{\beta} \left(1 - \frac{m^2 h^2}{X^2}\right) \right] \right. \\ & \left. - \frac{9m^2 h^2}{2X^2 (X^2 - m^2 h^2)} \left(\frac{3}{2} + \frac{m^2 h^2}{2X^2}\right) \right\}, \end{aligned} \quad (55)$$

where we have assumed $m \gg 1$, since these are the values of interest for the tidal torque (see GT79). This expression is valid even for m larger than or very large compared to $1/h$, and whatever the values of b_1, b_2, c_1, d_1 and d_2 compatible with β and h being constant and provided they are not large compared to unity. Note that the expression above can also be seen as an expansion around the corotation radius, which corresponds to $X = 0$.

5.4.2 Calculation of the turning points:

The turning points are the radii where $\mathcal{K} = 0$. We solve this equation numerically and display the results in figure 1, where we plot $(r - r_p)/H$ (where $H \equiv c/\Omega$) as a function of m for the turning points located beyond corotation, and for $\beta = 0.1, 1$ and 10 and $H/r = 0.03$. The outer magnetic resonance is also represented. To each of these outer turning points and resonance corresponds an inner turning point or resonance located at the same distance from corotation to first order in H/r or $1/m$. Similar plots are obtained for other values of H/r .

Artymowicz (1993) has calculated that, in a nonmagnetized disc, the location of the turning points is given by (his eq. [39]):

$$\frac{r - r_p}{H} = \frac{2}{3mh_L} \sqrt{1 + m^2 h_L^2},$$

so that, for $m \rightarrow \infty$, the distance to corotation is $2H/3$.

In a magnetized, we identify up to three turning points, that we label R1, R2 and R3:

- (i) The outermost turning point R1 coincides with the nominal Lindblad resonance for small values of m . When $m \rightarrow \infty$, its distance to corotation is $2H/3$ for $\beta \geq 1$ (like in the nonmagnetic case) and $2H/(3\sqrt{\beta})$ for $\beta \leq 1$, i.e. $2H'/3$ with $H' \equiv v_A/\Omega$.
- (ii) The intermediate turning point R2 is located at a distance from corotation equal to $2H/(3\sqrt{\beta})$ for $\beta \geq 1$ and $2H/3$ for $\beta \leq 1$.
- (iii) The innermost turning point R3 exists only above some critical value of m , m_{crit} , which depends on β and H/r . Interpolation of the numerical results gives $m_{\text{crit}} \simeq 1.5\sqrt{\beta} \times r/H$. When $m \rightarrow \infty$, the distance of this turning point to corotation is $2H/(3\sqrt{\beta+1})$, i.e. it coincides with the magnetic resonance. For either $\beta \ll 1$ or $\beta \gg 1$, R2 and R3 merge at large m .

In figure 1, the shaded areas indicate where the waves are evanescent (i.e. $\mathcal{K} < 0$). In contrast to the nonmagnetic case, there is a region inside the outermost turning points where waves propagate. This region moves toward the corotation radius and decreases in size as β increases. It disappears altogether for infinite β . Note that the magnetic resonances are contained within this region, so that the singular slow modes excited at the magnetic resonances can propagate.

Since waves do not propagate around corotation for $m > m_{\text{crit}}$, we expect a torque cutoff at large m like in the nonmagnetic case.

We can check whether waves propagate or not around corotation by taking the limit $X \rightarrow 0$ (i.e. $r \rightarrow r_p$) in the expression (55) above. In the nonmagnetic case ($\beta \rightarrow \infty$):

$$\frac{m^2}{\mathcal{A}_2^2} \mathcal{K} \rightarrow -1 - \frac{7}{4m^2 h_L^2}.$$

Since this is negative, the waves are evanescent around corotation in that case. When β is finite:

$$\frac{m^2}{\mathcal{A}_2^2} \mathcal{K} \rightarrow \frac{(m^2 h_L^2)^2}{X^4} \left(-\frac{1}{\beta} + \frac{9}{4m^2 h_L^2} \right).$$

This is positive when $m < m_{\text{crit}}$ with $m_{\text{crit}} = 3\sqrt{\beta}/(2h_L)$, so that waves propagate around corotation for these values of m . Note that the value of m_{crit} found by interpolation of the numerical results agrees perfectly with the analytical expression.

6 TIDAL TORQUE

6.1 Expression for the torque

In the linear regime, the net torque exerted by the planet on the disc between the radii r_1 and r_2 is:

$$\mathbf{T}(r_1, r_2) = \sum_{m=0}^{\infty} \mathbf{T}_m(r_1, r_2),$$

with:

$$\mathbf{T}_m(r_1, r_2) = - \int_{r_1}^{r_2} \int_0^{2\pi} \text{Re} \left[\Sigma + \Sigma'_m e^{im(\varphi - \Omega_p t)} \right] \mathbf{r} \times \text{Re} \left[\nabla \left(\Psi'_m e^{im(\varphi - \Omega_p t)} \right) \right] r d\varphi dr. \quad (56)$$

Because of the φ -periodicity, the first-order term is zero and the torque has only a z -component which can be written as:

$$T_m(r_1, r_2) = 2\pi \int_{r_1}^{r_2} \frac{dT_m}{dA} r dr \quad (57)$$

where, following KP93, we have defined the “torque density”:

$$\frac{dT_m}{dA} \equiv \frac{m}{2} \text{Im} \left(\Sigma'^* \Psi'_m \right). \quad (58)$$

The asterisk denotes the complex conjugate.

In a nonmagnetized disc, another useful quantity is the angular momentum flux:

$$F_m(r) = \Sigma r^2 \int_0^{2\pi} \text{Re} \left[v'_{m\varphi} e^{im(\varphi - \Omega_p t)} \right] \text{Re} \left[v'_{mr} e^{im(\varphi - \Omega_p t)} \right] d\varphi, \quad (59)$$

which can also be written under the form:

$$F_m(r) = \pi \Sigma r^2 \text{Re} \left(v'_{mr} v'^*_{m\varphi} \right). \quad (60)$$

In a nonmagnetized disc, inside the Lindblad resonances and away from corotation, the response of the disc is non wave-like and in phase with the perturbation, so that $\Sigma_m^* \Psi_m'$ is real. Outside the Lindblad resonances, the wavelength of the perturbation is small compared to the scale on which the perturbing potential varies so that $r \Sigma_m^* \Psi_m'$ integrated over radius is small. Therefore, most of the contribution to the torque comes from the resonances (Lynden-Bell & Kalnajs 1972, GT79). There are two contributions to the total torque. These are the Lindblad torque, which is equal to the angular momentum advected through the disc, and the corotation torque, which accumulates at the corotation resonance (GT79) and is associated with a discontinuity of the angular momentum flux there.

In the presence of a magnetic field, it is not clear it is possible to calculate the torque separately at the different turning points, because the scale on which the disc response varies there may become larger than the distance between the turning points. In addition, the torque exerted around corotation for the values of m for which waves propagate there may be significant, as the scale on which the perturbing potential varies and that on which the disc response varies may be similar. The total torque will then be calculated numerically.

However, an asymptotic form of the torque density at the magnetic resonances can be obtained, and this is done in the next subsection.

6.2 Torque at the magnetic resonances

The torque density in the vicinity of a magnetic resonance is, from equation (58) and with $\Sigma_m' = \Sigma W_m / c^2$ given by equation (49):

$$\frac{1}{(\Sigma r^2 \Omega^2)_{r_M}} \frac{dT_m^M}{dA} = \left(\frac{\Psi_m'}{r^2 \Omega^2} \right)_{r_M} \frac{m}{2\beta_M} \operatorname{Im} \left(\frac{C_\epsilon^*}{x - i\gamma} \right), \quad (61)$$

$$= \left(\frac{\Psi_m'}{r^2 \Omega^2} \right)_{r_M} \frac{m}{2\beta_M} \frac{x \operatorname{Im}(C_\epsilon^*) + \gamma \operatorname{Re}(C_\epsilon^*)}{x^2 + \gamma^2}. \quad (62)$$

To get the torque exerted over a magnetic resonance, we integrate the torque density over the width Δr of the resonance, i.e. from $r_M - \Delta r/2$ to $r_M + \Delta r/2$. Note that $\Delta x \equiv \Delta r/r_M \sim \gamma$. Equation (49) has been used to derive the above expression for the torque density. Therefore, only if Δx , and hence γ , is small compared to h_M can this expression be used to calculate the torque over the resonance. When this condition is satisfied, the torque can be written as:

$$\frac{T_m^M}{(\Sigma r^4 \Omega^2)_{r_M}} \sim \operatorname{Re}(C_\epsilon) \frac{2\pi m}{\beta_M} \left(\frac{\Psi_m'}{r^2 \Omega^2} \right)_{r_M} \arctan \frac{\Delta x}{2\gamma}. \quad (63)$$

with $\arctan[\Delta x/(2\gamma)] \sim \pi/2$ if Δx is a few times γ .

Here we have assumed that the resonance were symmetrical around r_M , so that the term proportional to $\operatorname{Im}(C_\epsilon^*)$ in equation (62) gives no contribution. Since the integral over the term proportional to $\operatorname{Re}(C_\epsilon^*)$ converges (does not depend on the width of the resonance), the torque we obtain can be considered as a point-like contribution from the resonance, similar to the corotation torque in the nonmagnetic case. However, the resonance may not be symmetrical, in which case the term proportional to $\operatorname{Im}(C_\epsilon^*)$ gives a global contribution, which does depend on the extent of the resonance. We will see below that the torque around the magnetic resonances is indeed dominated by this global contribution, and not by the point-like torque.

Since $\operatorname{Re}(C_{+1}) = -\operatorname{Re}(C_{-1})$, the torque derived above has opposite sign at the inner and outer magnetic resonances.

To know the amplitude and the sign of T_m^M we need to calculate $\operatorname{Im}(C_\epsilon)$. This cannot be done from the local analysis presented in section 5.3, as only the solutions of the homogeneous equation determine the behaviour of the disc response at the magnetic resonances. The solutions obtained around the magnetic resonances are valid only for $|r - r_M| \ll H$ and therefore cannot be matched to the WKB solutions calculated in section 5.2. The constants C_ϵ will then be calculated by matching the numerical and analytical solutions, and the asymptotic form of the torque density given by equation (61) will be used to obtain a precise value of the torque at the magnetic resonances.

7 NUMERICAL CALCULATIONS

In order to calculate the tidal torque exerted by the planet on the disc, we have solved the second-order linearized differential equation (26) numerically.

7.1 Numerical scheme

The numerical scheme we have used is similar to that presented by KP93.

The coefficients Ψ_m' of the Fourier decomposition of the potential (see eq. [12]) are calculated using the recurrence formulae between the generalized Laplace coefficients (see the appendix of KP93, which unfortunately contains several typos).

Equation (26) is then integrated using the fifth-order Runge-Kutta procedure with adaptative stepsize control given by Press et al. (1992) from the disc inner radius r_{in} to its outer radius r_{out} . Note that KP93 started the integration at the

corotation resonance and shot toward the boundaries. This procedure would not be appropriate here as in the presence of a magnetic field there is a resonance on each side of corotation. For a given value of m , we first compute two independent solutions $\xi_{mr,1}$ and $\xi_{mr,2}$ of the homogeneous equation, and one particular solution $\xi_{mr,p}$ of the inhomogeneous equation starting with random initial values. The general solution is then given by $\xi_{mr} = \xi_{mr,p} + c_1\xi_{mr,1} + c_2\xi_{mr,2}$, where c_1 and c_2 are constants which depend on the boundary conditions.

To calculate c_1 and c_2 , we use the WKB solution of the equation, which should be valid at r_{in} and r_{out} if the boundaries are far enough from corotation. Then, at these locations, $d\xi_{mr}/dr = ik\xi_{mr}$, where k is given by equation (37). Since the physical solutions are outgoing waves, we take $k > 0$. The group velocity is then positive (negative) outside (inside) corotation. These two boundary conditions yield two algebraic equations for c_1 and c_2 (see eq. [24] of KP93) which can be solved to find these coefficients.

To get better numerical accuracy, we repeat the procedure taking for the starting value of the particular solution $\xi_{mr,p}$ the value of ξ_{mr} calculated at $r = r_{in}$ with the above coefficients c_1 and c_2 . This leads to $\xi_{mr,p}$ converging toward the full solution ξ_{mr} . When recalculating c_1 and c_2 after one iteration we indeed verify that these two constants are very close to zero. This procedure prevents large cancellation between $\xi_{mr,p}$ and the general solutions of the homogeneous equation.

Note that KP93 found the WKB approximation not to be accurate enough for the boundary conditions, and they accordingly took into account the amplitude as well as the phase variation of the WKB solution. We found that we could reproduce their results without having to go beyond the WKB approximation.

Once ξ_{mr} is known, W'_m and $v'_{m\varphi}$ can be calculated from equations (32) and (34), $v'_{mr} = im\sigma\xi_{mr}$, and the torque density dT_m/dA is given by equation (58). To calculate the total torque T_m exerted by the planet on the disc, we integrate dT_m/dA over the disc surface (see eq. [57]).

7.2 Numerical results

The planet potential softening length is set to $r_0 = 10^{-4}r_p$. Note that in the presence of a magnetic field the results are insensitive to the value of r_0 provided it is small enough, since there is no singularity of the homogeneous equation at $r = r_p$, where the potential is singular. The Landau parameter is set to $\gamma = 10^{-6}$. As expected, the total torque does not depend on the value of γ provided it is small enough.

For $m \leq 5$, we integrate the equation from $r_{in} = 0.2r_p$ to $r_{out} = 5r_p$, whereas, for $m \geq 6$, we limit the range of integration from $r_{in} = 0.5r_p$ to $r_{out} = 1.5r_p$.

We assume that Σ , c and $r^2\langle B^2 \rangle$ vary like power laws of r . According to equations (22) and (31), we then have $\Sigma \propto r^{d_1}$, $c \propto r^{c_1}$ and $r^2\langle B^2 \rangle \propto r^{b_1}$. Then $d_2 = d_1(d_1 - 1)$ and $b_2 = (b_1 - 2)(b_1 - 1)$. Note that $H/r \sim c/(r\Omega) \propto r^{c_1+0.5}$ and $\beta \equiv c^2/v_A^2 \propto r^{2c_1+d_1-b_1+2}$. We comment that the values of the parameters we chose below may require a departure from Keplerian rotation that is second order in H/r to ensure hydrostatic equilibrium. This is here neglected, as in Ward (1986, 1997).

To simplify the discussion, we define the dimensionless quantities $\tilde{W}'_m = W'_m / (r_p^2\Omega_p^2)$, $\tilde{T}_m = T_m / (\Sigma_p r_p^4\Omega_p^2)$, $\tilde{T}_{m,D} = 2\pi(T_m/dA) / (\Sigma_p r_p^2\Omega_p^2)$ and $\tilde{F}_m = F_m / (\Sigma_p r_p^4\Omega_p^2)$, where the subscript p indicates that the quantity is taken at $r = r_p$. The numerical results presented in this section correspond to $M_p/M_* = 1$. Since $\Psi'_m/(r_p^2\Omega_p^2) \propto M_p/M_*$ (see section 4), then $\tilde{W}'_m \propto M_p/M_*$ and $\tilde{T}_m \propto (M_p/M_*)^2$.

7.2.1 Case $B = 0$

By setting $B = 0$, we have checked that we recover the KP93 results. In that case, the corotation torque is non zero if $d_1 \neq -1.5$ and corresponds to a discontinuity of the angular momentum flux at $r = r_p$. In figure 2, we plot \tilde{W}'_m , the angular momentum flux $\tilde{F}_m(r)$ at radius r and the torque $\tilde{T}_m(r_p, r)$ exerted by the planet on the disc between the radii r_p and r for $B = 0$, $d_1 = 0$, $c/(r_p\Omega_p) = 0.03$ ($c_1 = 0$) and $m = 10$. For comparison, we also plot the angular momentum flux corresponding to $d_1 = -1.5$ in the corotation region. The parameters used here are the same as those used by KP93 in their figures 2, 5 and 6, so that a direct comparison can be made. For $d_1 = 0$, the dimensionless corotation torque is about 102, whereas the dimensionless total torque $\tilde{T}_m(r_{in}, r_{out})$ is about 22, in very good agreement with the results displayed by KP93.

7.2.2 Case $B \neq 0$

We first consider the case $d_1 = 0$, $c/(r_p\Omega_p) = 0.03$ ($c_1 = 0$), $b_1 = 2$, $\beta = \text{const} = 1$ and $m = 10$. In figures 3, 4 and 5 we plot \tilde{W}'_m , $\tilde{T}_{m,D}$ and \tilde{T}_m versus radius. Note that the rapid variation of $\text{Re}(\tilde{W}'_m)$ at $r = r_p$ is due to the rapid variation of the potential there, not to a singularity of the homogeneous differential equation. We have matched W'_m obtained numerically with the analytical expression (49) in order to compute the constants C_ϵ . We find that $\text{Re}(C_{+1}) > 0$ whereas $\text{Re}(C_{-1}) < 0$. According to equation (63), the point-like torque exerted at the outer magnetic resonance is then negative whereas that exerted at the inner magnetic resonance is positive. This is in agreement with the curves shown in figure 4 around resonances. Figure 5 shows the total torque computed using the numerical form of the torque density. As a check, we have also calculated \tilde{T}_m by using the analytical expression (61) for the torque density around the resonances (represented by the dashed lines in the lower panels of fig. 4). In general the two calculations are in good agreement with each other, although in some cases the discrepancy may reach about 50% (the sign of the torque does not change however).

In figure 6, we plot the total torque \tilde{T}_m exerted by the planet on the disc versus m for different values of d_1 , c_1 and b_1 and for both $B = 0$ and $B \neq 0$. In the magnetic case, the value of β at r_p is taken to be 1. The cumulative torque \tilde{T} is obtained by summing up over m . We get an estimate by assuming \tilde{T}_m is constant in the intervals $20 \leq m \leq 24$, $25 \leq m \leq 29$ etc... and $\tilde{T}_m = 0$ for $m > 85$.

The values computed for $B = 0$ are in very good agreement with KP93. In this case, the cumulative torque exerted by the planet on the disc is positive, which means that the planet loses angular momentum and migrates inward. When the magnetic field is non zero though, \tilde{T} may become negative, with a subsequent outward planet migration. This occurs when b_1 is negative enough, i.e. when β increases fast enough with radius or, equivalently, when the magnetic field decreases fast enough with radius. For instance, when $d_1 = c_1 = 0$, $\tilde{T} < 0$ for $b_1 = -1$, i.e. $\beta \propto r^3$ or, equivalently, $\langle B^2 \rangle \propto r^{-3}$, and for $b_1 = 0$, i.e. $\beta \propto r^2$ or, equivalently, $\langle B^2 \rangle \propto r^{-2}$. Note that this variation needs only be *local*. When b_1 goes from positive to negative values, the cumulative torque, initially positive, then becomes negative passing through zero. Therefore migration is slowed down and then reversed.

In figure 7, we plot the one-sided torque exerted by the planet on the disc (i.e. the torque exerted inside and outside its orbit) versus m for $d_1 = 0$ and $c/(r_p\Omega_p) = 0.03$, i.e. $c_1 = 0$. These plots show that the one-sided torque has a larger amplitude when a magnetic field is present.

In figure 8 we plot the torque exerted between r_{in} and r versus r/r_p for $m = 10$, $d_1 = c_1 = 0$, $\beta(r_p) = 1$ and for $b_1 = 7, 2$ and -8 . This shows that the total torque becomes negative when b_1 is negative due to the contribution from the region inside the Lindblad resonances.

In table 1 we have listed the value of the torque exerted on different radii intervals in the disc for $m = 10$, $d_1 = 0$, $c/(r_p\Omega_p) = 0.03$ ($c_1 = 0$), $\beta(r_p) = 1$ and different values of b_1 . The torque exerted between the inner Lindblad resonance r_{ILR} and corotation r_p is negative, whereas that exerted between corotation and the outer Lindblad resonance r_{OLR} is positive. (Note that for $m = 10$ the Lindblad resonances coincide with the outermost turning points). We have found above that the point-like torque exerted at the inner magnetic resonance is positive whereas that exerted at the outer resonance is negative. Therefore, the torque is not dominated by the point-like contribution at the magnetic resonances, but is determined by the whole region around these resonances, where waves propagate for $m < m_{crit}$ (see also the discussion in section 6.2). When b_1 decreases, β increases outward faster, so that the magnetic field becomes less and less important outside the planet's orbit. Therefore the torque exerted between r_p and r_{OLR} , which is positive and tends to be negligible in the absence of a magnetic field, becomes less and less important. In contrast, the magnetic field becomes more important inside the orbit, where it gives rise to a negative torque. The net effect of decreasing b_1 is then to decrease the total torque. If the magnetic field is strong enough, the total torque exerted on the disc is dominated by the region inside the Lindblad resonances (which is closer to the planet than the regions outside these resonances), and it can then become negative for small enough values of b_1 .

Figure 9 shows the total torque exerted by the planet on the disc versus m for $d_1 = 0$, $c/(r_p\Omega_p) = 0.03$ ($c_1 = 0$), $b_1 = -1$, which correspond to $\beta \propto r^3$, and different values of $\beta(r_p)$. As we can see, the cumulative torque \tilde{T} is significantly decreased for values of $\beta(r_p)$ as large as 10^2 and becomes negative for values of $\beta(r_p)$ between 10^2 and 10.

The cumulative torque corresponding to $\beta(r_p) = 10^2$ becomes negative if, for the same parameters as above, d_1 is taken to be at least as large as unity, i.e. if Σ increases with radius at least as fast as linearly. This is because when d_1 increases β increases faster with radius, which favours the negative inner torque exerted near corotation. This effect can be seen in figure 6 by comparing the upper and middle panels, which show that the total torque corresponding to $d_1 = -1.5$ is larger than that corresponding to $d_1 = 0$ for $b_1 = -1$. Note that $d_1 > 0$ tends to favour the outer Lindblad resonance compared to the inner one, which results in a larger Lindblad torque (Ward 1986, 1997). The fact that the total torque actually decreases when d_1 increases means that the variations of Σ affect more significantly the torque exerted around the magnetic resonances than the Lindblad torque. (Note that the variations of the torque displayed in figure 6 when d_1 varies in the nonmagnetic case are mainly due to changes in the corotation torque).

An increase of c_1 (corresponding to c or, equivalently, H/r , increasing faster with radius) also results in a smaller total torque, as can be seen by comparing the upper and lower panels of figure 6. When c_1 gets larger, β increases faster with radius, which again lowers the torque exerted around the magnetic resonances. Also the Lindblad torque is reduced when c_1 gets larger (Ward 1986, 1997).

Figure 10 shows the effect of varying the value of $H/r \equiv c/(r\Omega)$ at $r = r_p$ for $m = 10$, $d_1 = 0$, $c_1 = 0$, $\beta(r_p) = 1$ and $b_1 = -1$ and 3. The total torque exerted on the disc tends to zero as H/r increases. This is because the resonances are further away from the planet when H/r is larger, so that the coupling between the perturbation and the tidal potential is weaker. For $b_1 = -1$, the torque is always negative and decreases as H/r decreases. For $b_1 = 3$, the torque is positive and maximum for some value of H/r (~ 0.03). It stays positive (and becomes smaller) as H/r increases, whereas it becomes negative for smaller values of H/r . This is because even though β increases with radius in that case, the region between the inner Lindblad resonance and corotation contributes to a larger magnitude of the torque than the region between corotation and the outer Lindblad resonances. This is also the case for $H/r = 0.03$ and $b_1 = 1$, as shown in table 1.

Note that what determines the sign of the torque is the gradient of β , not of the magnetic field itself, as only β enters into equation (26).

8 DISCUSSION AND CONCLUSION

We have calculated the linear torque exerted by a planet on a circular orbit on a disc containing a toroidal magnetic field. In contrast to the nonmagnetic case, there is no singularity at the corotation radius, where the frequency of the perturbation matches the orbital frequency. However, there are two new singularities on both sides of corotation, where the frequency of the perturbation in a frame rotating with the fluid matches that of a slow MHD wave propagating along the field line. These so-called *magnetic resonances* are closer to the planet than the Lindblad resonances. In addition, on each side of the planet, there are two turning points located beyond the magnetic resonance. One of them coincides with the Lindblad resonance. For values of m larger than some critical value m_{crit} , there is a third turning point between the magnetic resonance and corotation, on each side of the planet. Like in the nonmagnetic case, waves propagate outside the outermost turning points. But here they also propagate inside the intermediate turning points when $m < m_{\text{crit}}$, or between the intermediate and innermost turning points when $m > m_{\text{crit}}$ (see figure 1). The singular modes excited at the magnetic resonances can therefore propagate.

There is a significant torque exerted on the region of the disc inside the outermost turning points (which coincide with the Lindblad resonances for the values of m of interest). Like the Lindblad torque, this torque is negative inside the planet's orbit and positive outside its orbit. The whole region around corotation, not just a narrow zone around the magnetic resonances, contribute to this torque. In other words, the magnetic resonances contribute to a global, not a point-like, torque. Since these resonances are closer to the planet than the Lindblad resonances, they couple more strongly to the tidal potential. Therefore, the torque exerted around the magnetic resonances dominate over the Lindblad torque if the magnetic field is large enough. If in addition $\beta \equiv c^2/v_A^2$ increases fast enough with radius, the outer magnetic resonance becomes less important (it disappears altogether when there is no magnetic field outside the planet's orbit) and the total torque is then negative, dominated by the inner magnetic resonance. This corresponds to a positive torque on the planet, which leads to outward migration.

The amount by which β has to increase outward for the total torque exerted on the disc to be negative depends mainly on the magnitude of β . We have found that for $\beta = 1$ at corotation, the cumulative torque (obtained by summing up the contributions from all the values of m) exerted on the disc is negative when β increases at least as fast as r^2 . If $\beta \propto r^3$, the cumulative torque becomes negative for values of $\beta(r_p)$ between 10^2 and 10, whereas it is negative for $\beta(r_p) = 10^2$ if $\beta \propto r^4$.

The migration timescales that correspond to the torques calculated above are rather short. The orbital decay timescale of a planet of mass M_p at radius r_p is $\tau = M_p r_p^2 \Omega_p / |T|$, where T is the cumulative torque exerted by the planet on the disc. Remembering that $T \propto (M_p/M_*)^2$, we get:

$$\tau(\text{yr}) = 4.3 \times 10^9 \left(\frac{M_p}{M_\oplus} \right)^{-1} \left(\frac{\Sigma_p}{100 \text{ g cm}^{-2}} \right)^{-1} \left(\frac{r_p}{1 \text{ au}} \right)^{-1/2} \tilde{T}^{-1}. \quad (64)$$

In a standard disc model, $\Sigma \sim 100\text{--}10^3 \text{ g cm}^{-2}$ at 1 au (see, for instance, Papaloizou & Terquem 1999). Therefore, $\tau \sim 10^5\text{--}10^6 \text{ yr}$ for a one earth mass planet at 1 au in a nonmagnetic disc, as $\tilde{T} \sim 10^3$ in that case (see fig. 6). This is in agreement with Ward (1986, 1997). In a magnetic disc, $|\tilde{T}|$ may become larger, leading to an even shorter migration timescale (note that given the limited accuracy of the numerical scheme used, as indicated in section 7.2.2, only orders of magnitude for the migration timescale are obtained here). However, it is important to keep in mind that these timescales are *local*. Once the planet migrates outward out of the region where β increases with radius, it may enter a region where β behaves differently and then resume inward migration for instance. Such a situation would be expected to occur in a turbulent magnetized disc in which the large scale field structure changes sufficiently slowly.

Unless the magnetic field is above equipartition, it is unstable by the magnetorotational instability (Balbus & Hawley 1991, 1998 and references therein), the saturated nonlinear outcome of which is MHD turbulence. In a turbulent magnetized disc, the main component of the field is toroidal, as shown by numerical simulations (Hawley, Gammie & Balbus 1995; Brandenburg et al. 1995). Global simulations have also shown that the turbulence saturates at a level corresponding to $\beta \sim 100$ if there is no mean flux or to lower values of β if there is a mean flux (Hawley 2001; Steinacker & Papaloizou 2002). Also, substantial spatial inhomogeneities are created by radial variations of the Maxwell stress (Hawley 2001; Steinacker & Papaloizou 2002), so that the field may display significant gradients. On the basis of the work presented here, we are led to speculate that in such a disc the planet would suffer alternately inward and outward migration, or even no migration at all. It would then oscillate back and forth in some region of the disc, or undergo some kind of diffusive migration, either outward or inward depending on the field gradients encountered. Note however that in a turbulent disc the magnetic field may vary locally on timescales shorter than the timescales needed to establish the type of tidal response assumed in this paper.

It has been pointed out that protoplanetary discs may be ionized enough for the magnetic field to couple to the matter only in their innermost and outermost parts (Gammie 1996; Fromang, Terquem & Balbus 2002). A planet forming at around one astronomical unit, where the ionization fraction is very low, would then migrate inward on the timescale calculated by Ward (1986, 1997) until it reaches smaller radii where the field is coupled to the matter. At this point, there would be a magnetic field inside the planet's orbit but not outside its orbit. The torque on the planet would then reverse, and outward migration would occur. However, as soon as the planet would re-enter the nonmagnetic region, inward migration would resume. Hence, the planet would stall at the border between the magnetic and nonmagnetic regions.

Inward migration in a magnetized disc may then either be very significantly slowed down, occur only on limited scales, or not occur at all. The planet would then be able to grow to become a terrestrial planet or the core of a giant planet.

When the planet becomes massive enough (about 10 earth masses), the interaction with the disc becomes nonlinear, with a gap being opened up around the planet's orbit. Because a rather strong torque is exerted in the vicinity of the planet in the presence of a magnetic field, a gap should open up more easily and be 'cleaner' in a turbulent magnetic disc than in a

similar laminar viscous disc. This seems to be in agreement with the numerical simulations of a giant planet in a turbulent disc performed by Nelson & Papaloizou (2002). Once the gap is completely cleared out, the effect of the magnetic resonances disappear as they are inside the edges of the gap (which coincide with the Lindblad resonances corresponding to $m \sim r/H$). The magnetic field may however still have an effect on the disc–planet interaction because of the turbulence it produces (Nelson & Papaloizou 2002).

We have focused here on a planet with a circular orbit. A planet on an eccentric orbit in a nonmagnetic disc usually suffers eccentricity damping, as in that case the corotation resonances, which damp the eccentricity, dominate over the Lindblad resonances, which excite it (Goldreich & Tremaine 1980; Papaloizou, Nelson & Masset 2001). This picture may change once a magnetic field is introduced. The effect of a magnetic field on the eccentricity of a planet will be studied in another paper.

ACKNOWLEDGEMENT

It is a pleasure to thank Steven Balbus and John Papaloizou for their advice, encouragement, and many valuable suggestions and discussions. I am grateful to John Papaloizou for his comments on an early draft of this paper which led to significant improvements.

REFERENCES

Abramowitz M., & Stegun I. A., 1972, *Handbook of Mathematical Functions* (New York: Dover)
 Artymowicz P., 1993, *ApJ*, 419, 155
 Balbus S. A., & Hawley J. F., 1991, *ApJ*, 376, 214
 Balbus S. A., & Hawley J. F., 1998, *Rev. Mod. Phys.*, 70, 1
 Bodenheimer P., 1998, in *Brown dwarfs and extrasolar planets*, eds R. Rebolo, E. L. Martin, & M. R. Zapatero Osorio (ASP Conference Series, vol. 134), p. 115.
 Bodenheimer P., Hubickyj O., & Lissauer J. J., 2000, *Icarus*, 143, 2
 Brandenburg A., Nordlund A., Stein R. F., & Torkelsson U., 1995, *ApJ*, 446, 741
 Chandrasekhar S., & Fermi E., 1953, *ApJ*, 118, 116
 Fromang S., Terquem C., & Balbus S. A., 2002, *MNRAS*, 329, 18
 Gammie C. F., 1996, *ApJ*, 457, 355
 Goldreich P., & Tremaine S., 1979, *ApJ*, 233, 857 (GT79)
 Goldreich P., & Tremaine S., 1980, *ApJ*, 241, 425
 Hawley J. F., 2001, *ApJ*, 554, 534
 Hawley J. F., Gammie C. F., & Balbus S. A., 1995, *ApJ*, 440, 742
 Korycansky D. G., & Pollack J. B., 1993, *Icarus*, 102, 150 (KP93)
 Lin D. N. C., & Papaloizou J. C. B., 1979, *MNRAS*, 188, 191
 Lin D. N. C., & Papaloizou J. C. B., 1993, in *Protostars and Planets III*, eds. E. H. Levy, & J. I. Lunine (Tucson: University of Arizona Press), p. 749
 Lynden-Bell D., & Kalnajs A. J., 1972, *MNRAS*, 157, 1
 Malhotra R., 1993, *Nature*, 365, 819
 Murray N., Hansen B., Holman M., & Tremaine S., 1998, *Science*, 279, 69
 Narayan R., Goldreich P., & Goodman J., 1987, *MNRAS*, 228, 1
 Nelson R. P., & Papaloizou J. C. B., 2002, *MNRAS*, submitted
 Papaloizou J. C. B., 2002, *A&A*, 388, 615
 Papaloizou J. C. B., & Larwood J. D., 2000, *MNRAS*, 315, 823
 Papaloizou J. C. B., & Lin D. N. C., 1984, 285, 818
 Papaloizou J. C. B., Nelson R. P., & Masset F., 2001, *A&A*, 366, 263
 Papaloizou J. C. B., & Terquem C., 1999, *ApJ*, 521, 823
 Papaloizou J. C. B., & Terquem C., 2001, *MNRAS*, 325, 221
 Press W. H., Flannery B. P., Teukolsky S. A., & Vetterling W. T., 1992, *Numerical Recipes: The Art of Scientific Computing* (Cambridge: Cambridge Univ. Press), 3rd ed.
 Rasio F. A., & Ford E. B., 1996, *Science*, 274, 954
 Steinacker A., & Papaloizou J. C. B., 2002, *ApJ*, 571, 413
 Tagger M., Henriksen R. N., Sygnet J. F., & Pellat R., 1990, *ApJ*, 353, 654
 Terquem C., Papaloizou J. C. B., & Nelson R. P., 2000, in *From Dust to Terrestrial Planets*, eds W. Benz, R. Kallenbach, & G. W. Lugmair (Kluwer: Dordrecht), p. 323
 Ward W. R., 1986, *Icarus*, 67, 164
 Ward W. R., 1989, *ApJ*, 336, 526
 Ward W. R., 1997, *Icarus*, 126, 261
 Weidenschilling S. J., & Marzari F., 1996, *Nature*, 384, 619

b_1	$\tilde{T}_m(r_{in}, r_{ILR})$	$\tilde{T}_m(r_{ILR}, r_p)$	$\tilde{T}_m(r_p, r_{OLR})$	$\tilde{T}_m(r_{OLR}, r_{out})$	Total torque \tilde{T}_m
8	-172	-110	624	194	536
7	-171	-153	553	186	415
3	-165	-305	408	208	146
2	-163	-344	377	209	79
1	-160	-385	333	211	-1
0	-158	-423	298	217	-66
-1	-154	-463	263	217	-137
-3	-155	-570	184	217	-324
-5	-145	-641	129	225	-432
-8	-105	-645	69	225	-456
	-126	-333	310	170	21

Table 1. Torque $\tilde{T}_m(r_1, r_2)$ exerted by the planet on the disc between the radii r_1 and r_2 in units $\Sigma_p r_p^4 \Omega_p^2$ for different values of b_1 and for $m = 10$, $d_1 = 0$, $c/(r_p \Omega_p) = 0.03$ ($c_1 = 0$) and $\beta(r_p) = 1$. The radii r_1 and r_2 are either the disc inner radius r_{in} , the inner Lindblad resonance r_{ILR} , the corotation radius r_p , the outer Lindblad resonance r_{OLR} or the disc outer radius r_{out} . For comparison, the last line shows the torques in the nonmagnetic case. As b_1 decreases, the torque exerted inside the Lindblad resonances becomes negative and dominant.

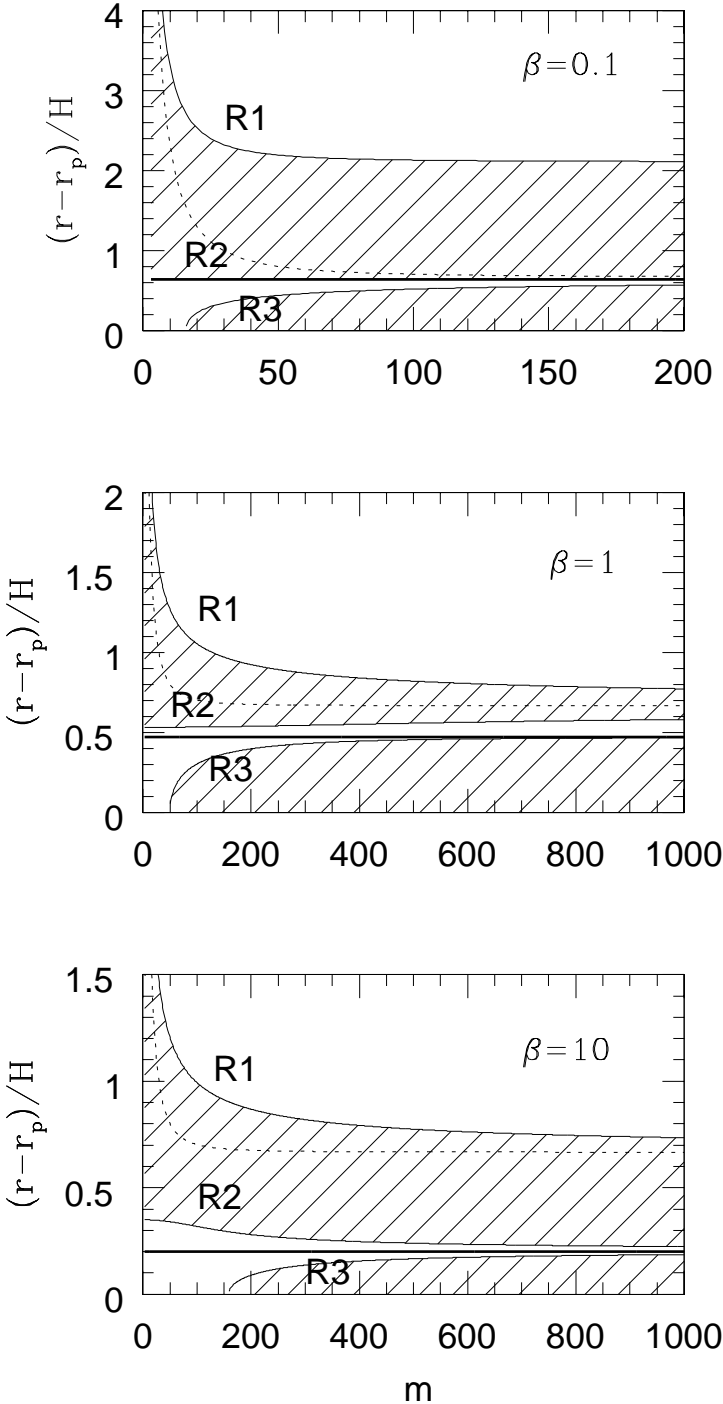


Figure 1. Distance of the outer turning points (thin solid lines) and magnetic resonance (thick bold lines) to corotation in units of $H \equiv c/\Omega$ versus m for $\beta = 0.1$ (upper plot), 1 (middle plot) and 10 (lower plot) and for $H/r = 0.03$. The turning points are labelled R1, R2 and R3. The shaded areas indicate the regions where the waves are evanescent. The location of the effective outer Lindblad resonance in a nonmagnetized disc is also represented (dashed lines). The inner turning points and resonance are obtained by reflection with respect to the x -axis.

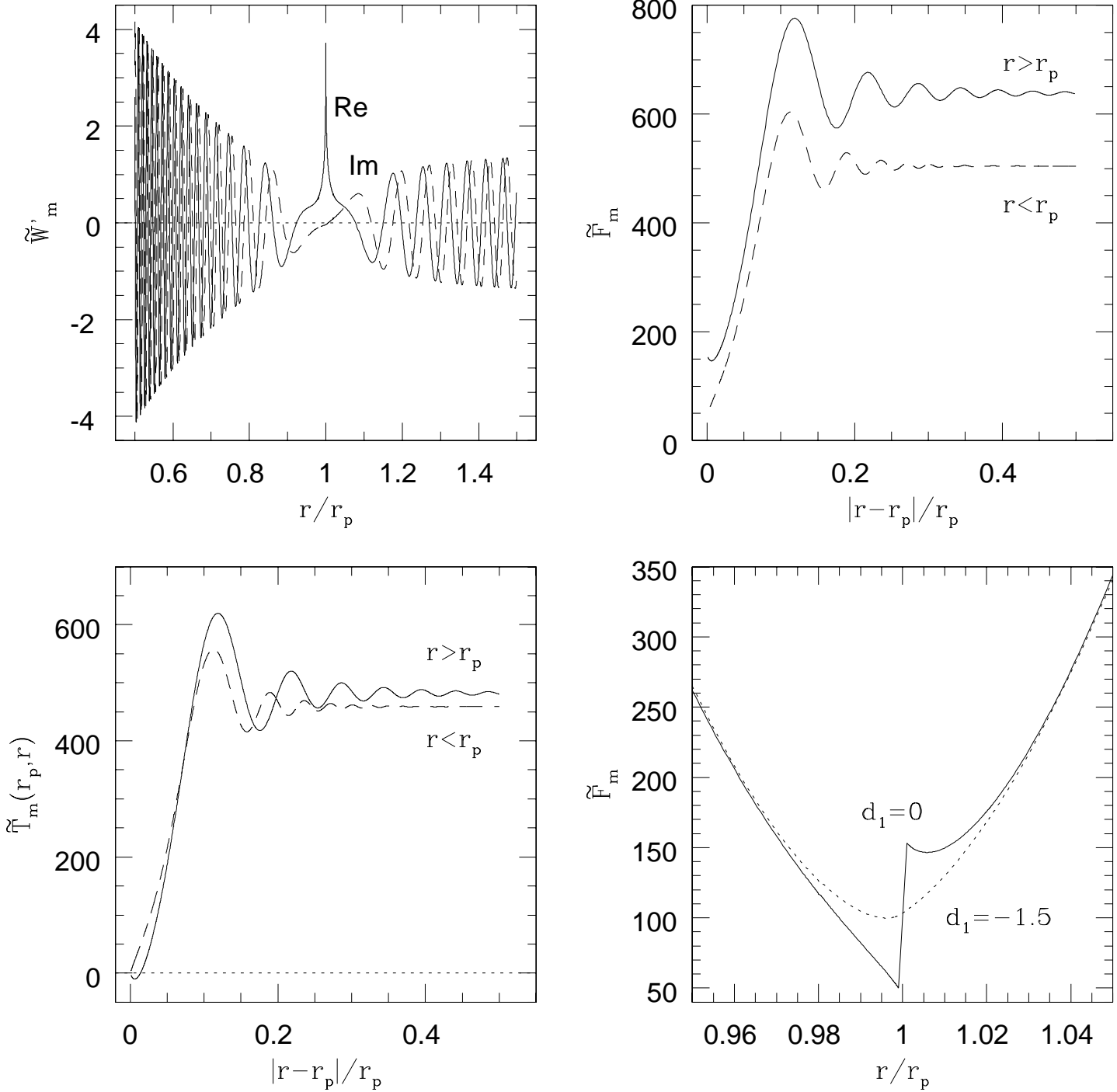


Figure 2. Results for $B = 0$, $d_1 \equiv d \ln \Sigma / d \ln r = 0$, $c / (r_p \Omega_p) = 0.03$ ($c_1 = 0$) and $m = 10$. *Upper left panel:* Real part (solid line) and imaginary part (dashed line) of \tilde{W}'_m versus r/r_p . *Lower left panel:* Tidal torque $\tilde{T}_m(r_p, r)$ exerted by the planet on the disc between the radii r_p and r versus $|r - r_p|/r_p$. The two curves correspond to $r > r_p$ (solid line) and $r < r_p$ (dashed line). *Upper right panel:* Angular momentum flux \tilde{F}_m versus $|r - r_p|/r_p$. The two curves correspond to $r > r_p$ (solid line) and $r < r_p$ (dashed line). *Lower right panel:* \tilde{F}_m versus r/r_p around corotation for $d_1 = 0$ (solid line) and -1.5 (dotted line).

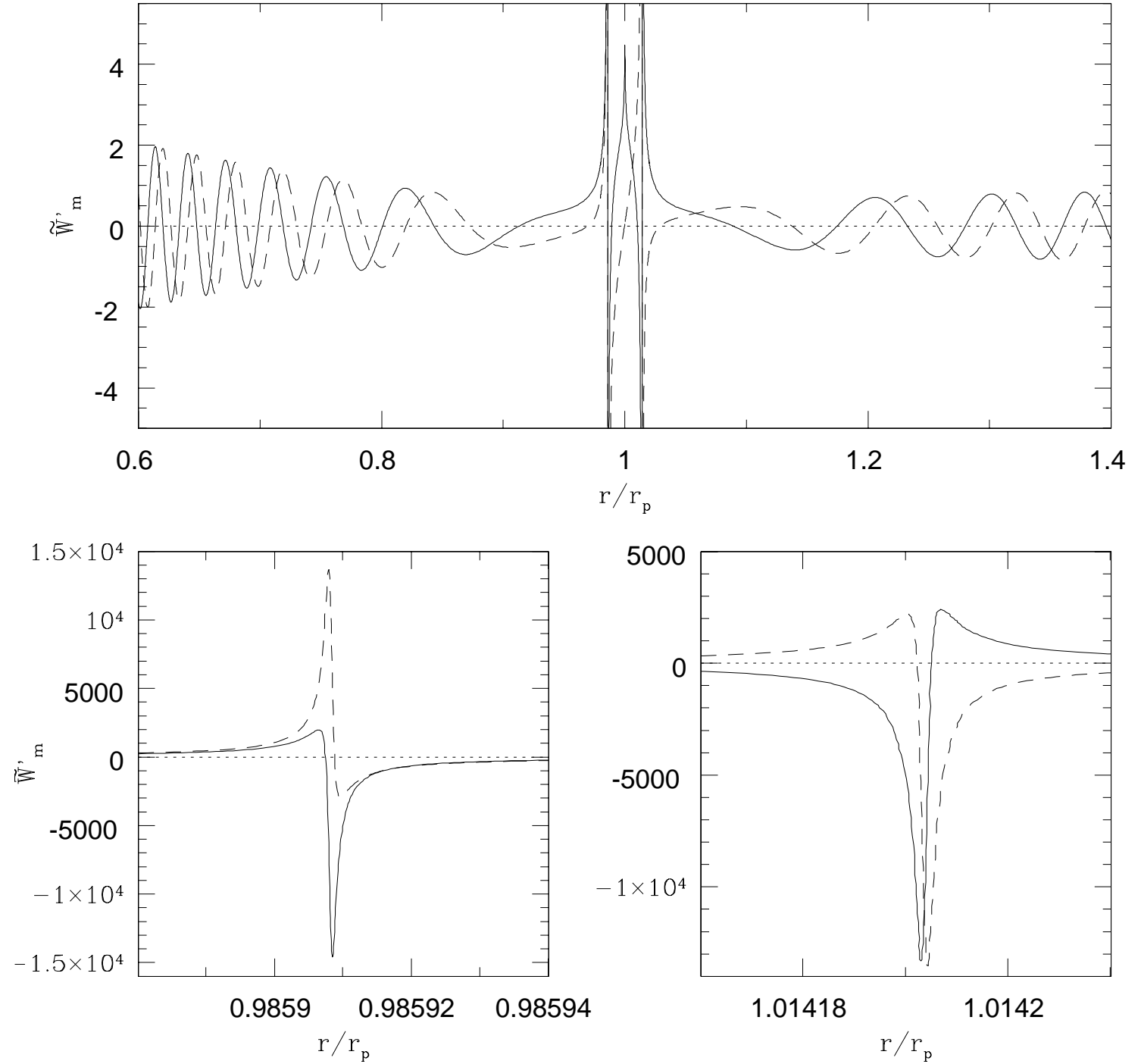


Figure 3. Results for $B \neq 0$: \tilde{W}'_m versus r/r_p for $d_1 = 0$, $c/(r_p\Omega_p) = 0.03$ ($c_1 = 0$), $b_1 = 2$, $\beta = \text{const} = 1$ and $m = 10$. Both the real part (solid line) and imaginary part (dashed line) are plotted. The two lower panels show a zoom on the magnetic resonances (left panel, inner resonance; right panel, outer resonance).

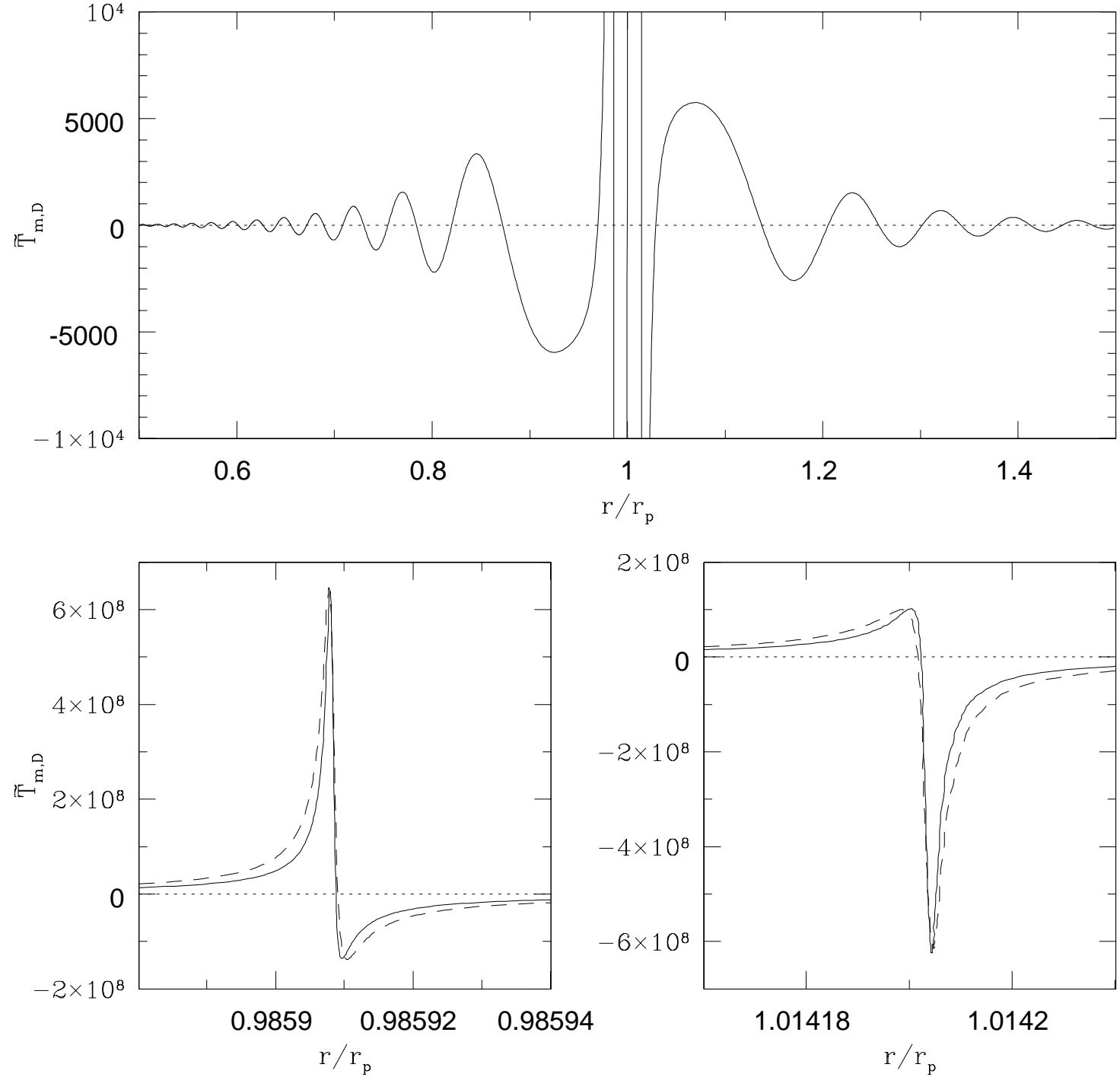


Figure 4. Torque density $\tilde{T}_{m,D}$ versus r/r_p for the same parameters as in fig. 3. The two lower panels show a zoom on the magnetic resonances (left panel, inner resonance; right panel, outer resonance). The dashed lines represent the fit given by equation (61), where the constants C_ϵ are calculated by matching W'_m obtained numerically with the analytical expression (49). The point-like torque exerted at the inner magnetic resonance is positive whereas that exerted at the outer magnetic resonance is negative.

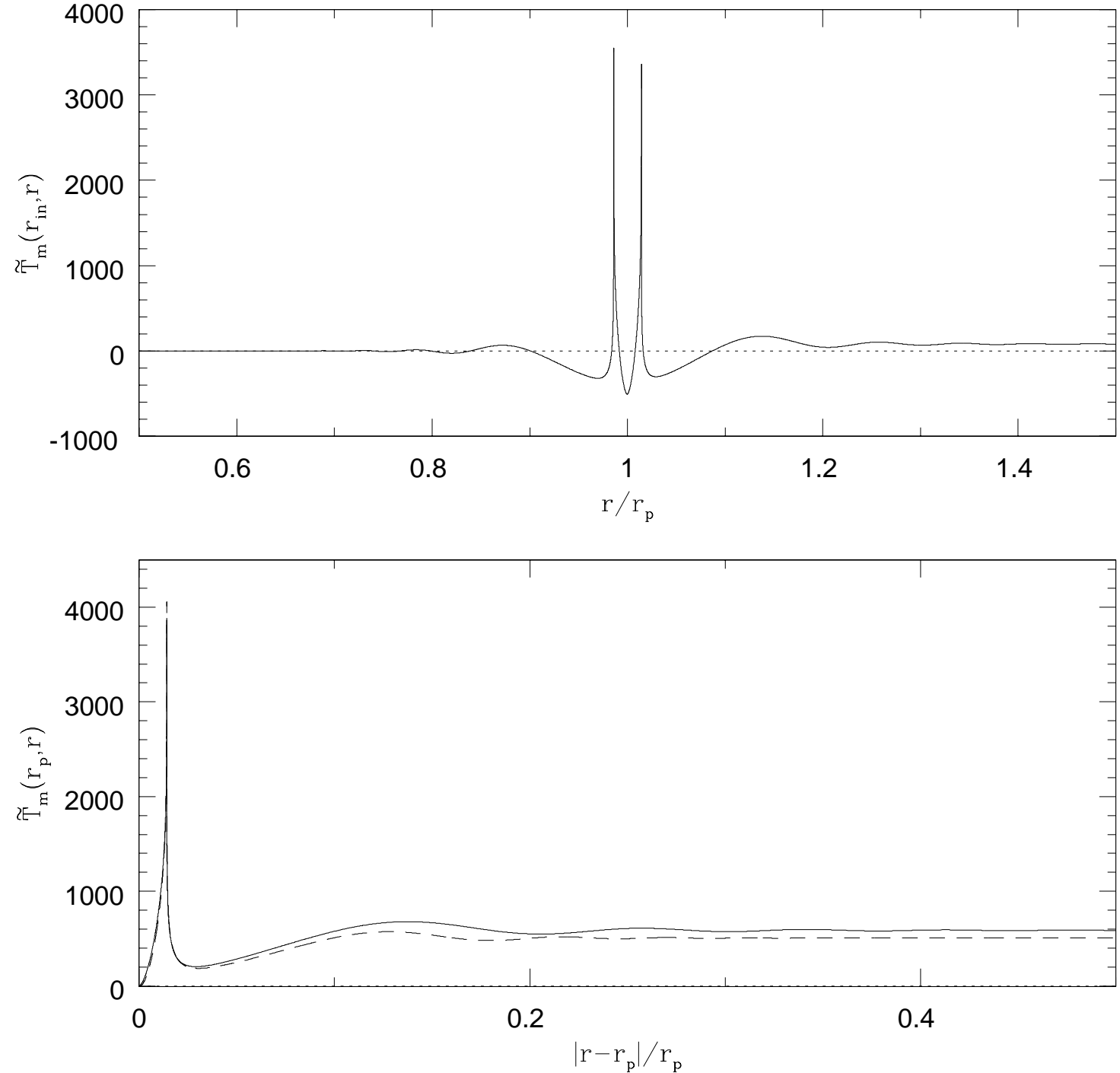


Figure 5. Torque \tilde{T}_m exerted by the planet on the disc for the same parameters as in fig. 3. The upper panel shows the torque exerted between the radii r_{in} and r versus r/r_p . The lower panel shows the torque exerted between the radii r_p and r versus $|r - r_p|/r_p$, for both $r > r_p$ (solid line) and $r < r_p$ (dashed line). Here the total torque on the disc is positive, like in the nonmagnetic case.

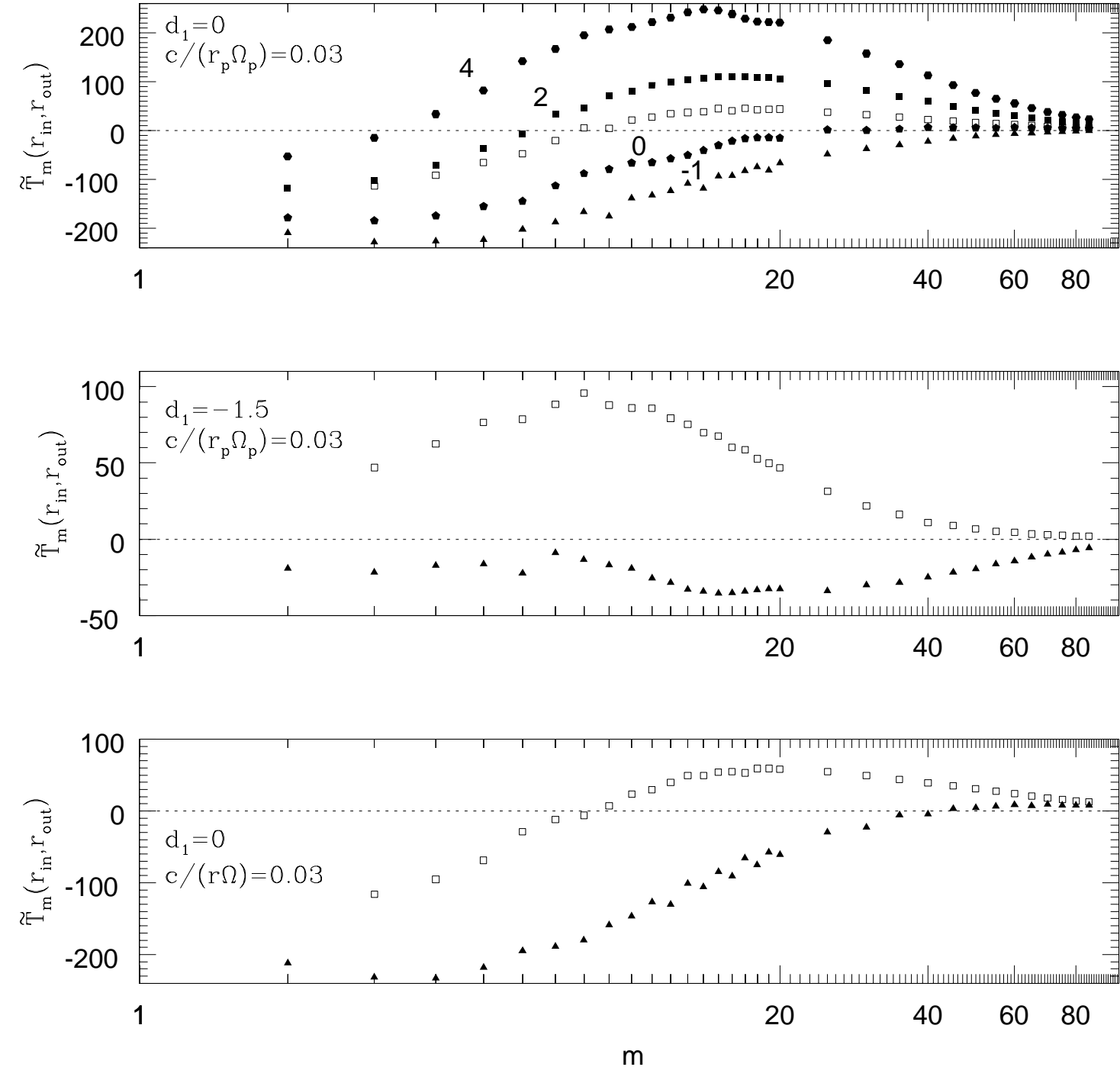


Figure 6. Total torque $\tilde{T}_m(r_{in}, r_{out})$ versus m for $d_1 = 0$ (upper and lower panels), and -1.5 (middle panel) and for $c/(r_p \Omega_p) = 0.03$, i.e. $c_1 = 0$ (upper and middle panels) and $c/(r \Omega) = 0.03$, i.e. $c_1 = -0.5$ (lower panel). The open squares correspond to $\beta = \infty$, i.e. $B = 0$. The filled symbols correspond to $\beta(r_p) = 1$ and $b_1 = -1$ (triangles), 0 (pentagons), 2 (squares) and 4 (hexagons), as indicated by the label on the curves. In the upper panel, an estimate of the cumulative torque gives $\tilde{T} = -3975, -1300, 4160$ and 9148 for $B \neq 0$ and $b_1 = -1, 0, 2$ and 4 , respectively, and $\tilde{T} = 1362$ for $B = 0$. In the middle panel, $\tilde{T} = -1768$ for $b_1 = -1$ and $\tilde{T} = 2051$ for $B = 0$. In the lower panel, $\tilde{T} = -2680$ for $b_1 = -1$ and $\tilde{T} = 2383$ for $B = 0$. A negative (positive) cumulative torque corresponds to the planet migrating outward (inward).

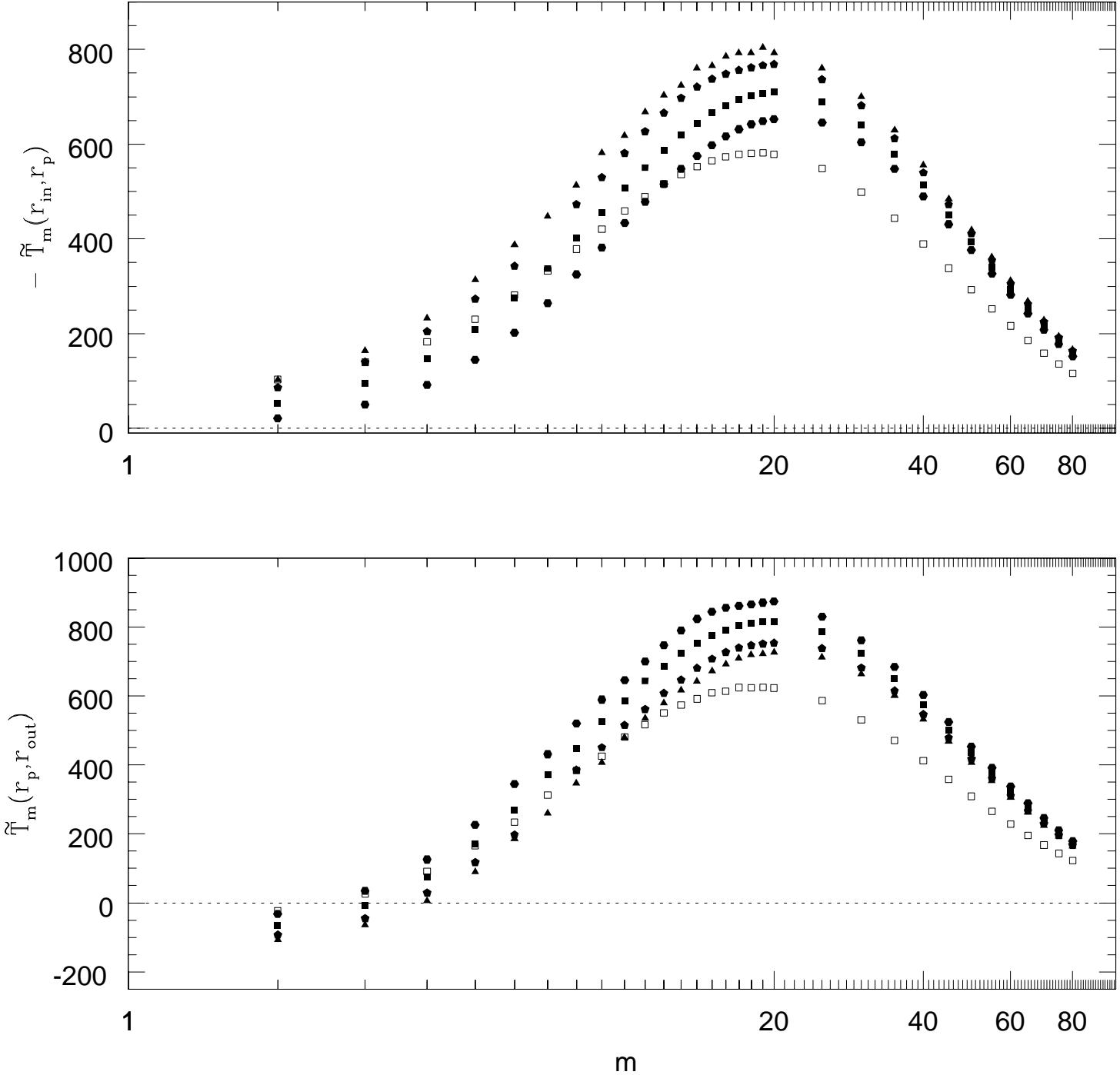


Figure 7. *Upper panel:* minus the torque exerted by the planet on the disc inside its orbit, $-\tilde{T}_m(r_{in}, r_p)$, versus m . *Lower panel:* torque exerted by the planet on the disc outside its orbit, $\tilde{T}_m(r_p, r_{out})$, versus m . The parameters are the same as in the upper panel of figure 6: $d_1 = 0$ and $c/(r_p\Omega_p) = 0.03$, i.e. $c_1 = 0$. Like in figure 6, the open squares correspond to $\beta = \infty$, i.e. $B = 0$, and the filled symbols correspond to $\beta(r_p) = 1$ and $b_1 = -1$ (triangles), 0 (pentagons), 2 (squares) and 4 (hexagons). An estimate of the cumulative torque for $m \leq 80$ gives $[\tilde{T}(r_{in}, r_p); \tilde{T}(r_p, r_{out})] = (-39531; 35560), (-37727; 36521), (-35442; 39535), (-32856; 42161)$ for $B \neq 0$ and $b_1 = -1, 0, 2$ and 4, respectively, and $(-28278; 29486)$ for $B = 0$. The one-sided torque has a larger amplitude when a magnetic field is present.

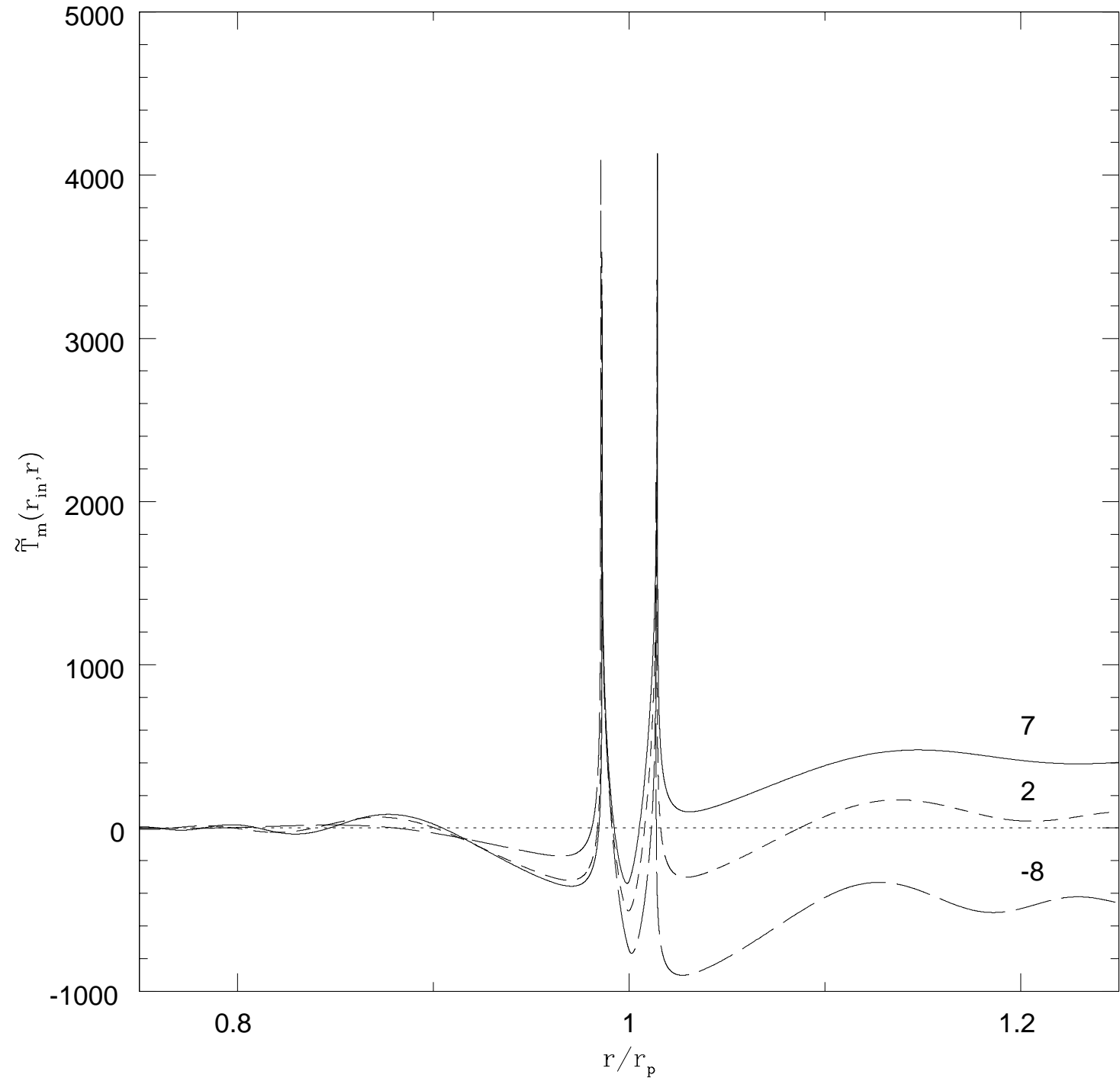


Figure 8. Torque $\tilde{T}_m(r_{in}, r)$ exerted between r_{in} and r versus r/r_p for $m = 10$, $d_1 = 0$, $c/(r_p\Omega_p) = 0.03$ ($c_1 = 0$), $\beta(r_p) = 1$ and $b_1 = 7$ (solid line), 2 (short-dashed line) and -8 (long-dashed line). As b_1 decreases, the torque exerted inside the Lindblad resonances becomes increasingly dominant and negative.

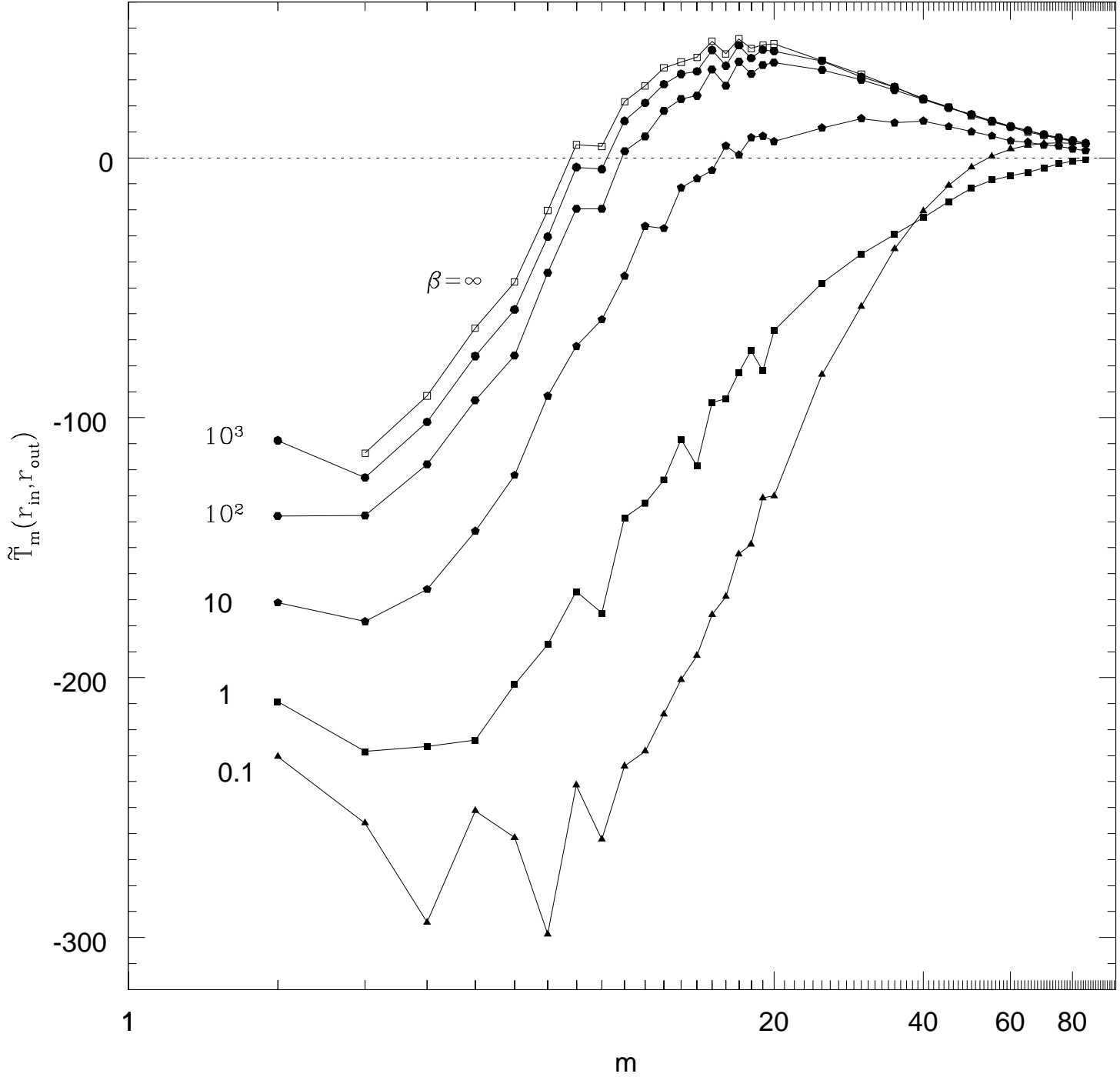


Figure 9. Total torque $\tilde{T}_m(r_{in}, r_{out})$ versus m for $d_1 = 0$ and $c/(r_p \Omega_p) = 0.03$ ($c_1 = 0$). The open squares correspond to $\beta = \infty$, i.e. $B = 0$. The filled symbols correspond to $b_1 = -1$ and $\beta(r_p) = 0.1$ (triangles), 1 (squares), 10 (pentagons) 10^2 (hexagons) and 10^3 (septagons). An estimate of the cumulative torque gives $\tilde{T} = 1362, 1129, 855, -508, -3975$ and -5483 for $\beta(r_p) = \infty, 10^3, 10^2, 10, 1$ and 0.1 , respectively. This shows that \tilde{T} is significantly reduced for values of β as large as 10^2 .

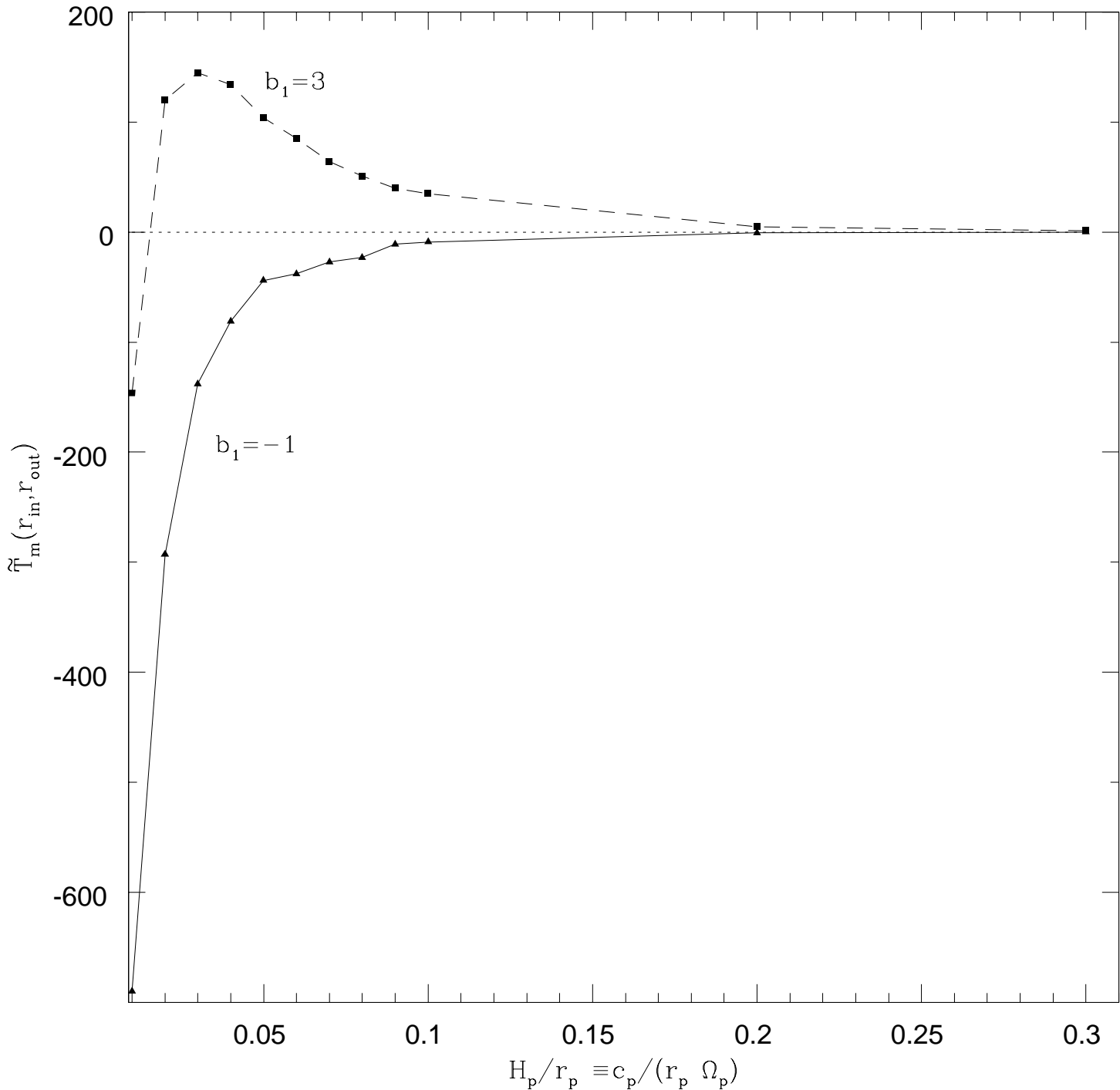


Figure 10. Total torque $\tilde{T}_m(r_{in}, r_{out})$ versus $H_p/r_p \equiv c_p/(r_p \Omega_p)$ (where the subscript 'p' indicates that the quantities are taken at $r = r_p$) for $m = 10$, $d_1 = 0$, $c_1 = 0$, $\beta(r_p) = 1$ and $b_1 = -1$ (solid line) and 3 (dashed line). The torque tends to zero as H/r increases.